Article

Sensitization of Ruthenium Nitrosyls to Visible Light via Direct Coordination of the Dye Resorufin: Trackable NO Donors for Light-Triggered NO Delivery to Cellular Targets

Michael J. Rose, Nicole L. Fry, Rebecca Marlow, Lindsay Hinck, and Pradip K. Mascharak

J. Am. Chem. Soc., **2008**, 130 (27), 8834-8846 • DOI: 10.1021/ja801823f • Publication Date (Web): 14 June 2008

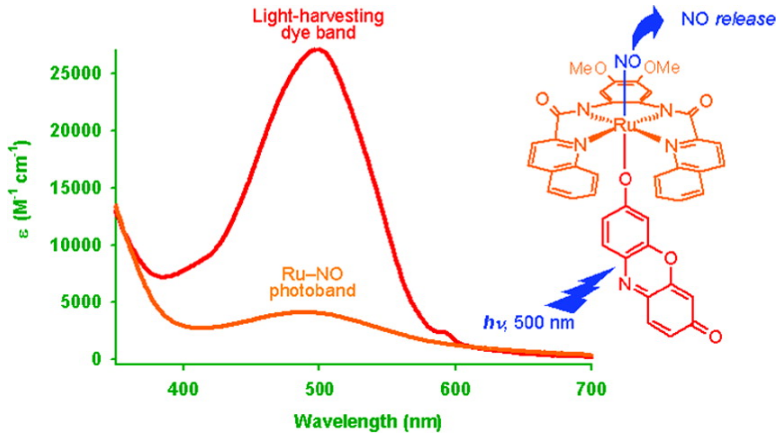

More About This Article

Additional resources and features associated with this article are available within the HTML version:

- Supporting Information
- Access to high resolution figures
- Links to articles and content related to this article
- Copyright permission to reproduce figures and/or text from this article

View the Full Text HTML

J|A|C|S
ARTICLES

Published on Web 06/14/2008

Sensitization of Ruthenium Nitrosyls to Visible Light via Direct Coordination of the Dye Resorufin: Trackable NO Donors for Light-Triggered NO Delivery to Cellular Targets

Michael J. Rose,[†] Nicole L. Fry,[†] Rebecca Marlow,[‡] Lindsay Hinck,[‡] and Pradip K. Mascharak*,[†]

Department of Chemistry and Biochemistry, University of California, Santa Cruz, California 95064 and Department of Molecular Cell and Developmental Biology, University of California, Santa Cruz, California 95064

Received March 14, 2008; E-mail: pradip@chemistry.ucsc.edu

Abstract: Three nitrosyl-dye conjugates, namely, [(Me_2bpb)Ru(NO)(Resf)] (**1-Resf**), [(Me_2bQb)Ru(NO)(Resf)] (**2-Resf**), and [(($OMe)_2$bQb)Ru(NO)(Resf)] (**3-Resf**) have been synthesized via direct replacement of the chloride ligand of the parent $\{Ru-NO\}^6$ nitrosyls of the type [(R_2byb)Ru(NO)(L)] with the anionic tricyclic dye resorufin (Resf). The structures of **1-Resf**−**3-Resf** have been determined by X-ray crystallography. The dye is coordinated to the ruthenium centers of these conjugates via the phenolato-O atom and is trans to NO. Systematic red shift of the d_π(Ru) → π^*(NO) transition of the parent nitrosyls [(R_2byb)Ru(NO)(L)] due to changes in R and y in the equatorial tetradentate ligand R_2byb^{2-} results in its eventual merge with the intense absorption band of the dye around 500 nm in **3-Resf**. Unlike the UV-sensitive parent [(R_2byb)Ru(NO)(L)] nitrosyls, these dye-sensitized nitrosyls rapidly release NO when exposed to visible light ($\lambda \geq 465$ nm). Comparison of the photochemical parameters reveals that direct coordination of the light-harvesting chromophore to the ruthenium center in the present nitrosyls results in a significantly greater extent of sensitization to visible light compared to nitrosyls with appended chromophore (linked via alkyl chains). **1-Resf** has been employed as a "trackable" NO donor to promote NO-induced apoptosis in MDA-MB-231 human breast cancer cells under the control of light. The results of this work demonstrate that (a) the d_π(Ru) → π^*(NO) transition (photoband) of $\{Ru-NO\}^6$ nitrosyls can be tuned into visible range via careful alteration of the ligand frame(s) and (b) such nitrosyls can be significantly sensitized to visible light by directly ligating a light-harvesting chromophore to the ruthenium center. The potential of these photosensitive nitrosyl-dye conjugates as (i) biological tools to study the effects of NO in cellular environments and (ii) "trackable" NO donors in photodynamic therapy of malignancies (such as skin cancer) has been discussed.

Introduction

The cytokine-induced elevated nitric oxide (NO) production by inducible nitric oxide synthase (*i*NOS) and associated cell death has drawn attention in recent years.[1–4] Relatively high (in μM range) concentrations of NO have been shown to limit tumor growth by promoting apoptosis (programmed cell death).[5–7] This occurs primarily via inhibition of mitochondrial cytochrome *c* oxidase (C*c*O), thereby arresting cellular respiration.[8,9] Several pro-apoptotic caspase signaling pathways are also activated.[10,11] These findings have prompted researchers to attempt site-specific delivery of high concentrations of NO from exogenous NO

[†] Department of Chemistry and Biochemistry.
[‡] Department of Molecular Cell and Developmental Biology.

(1) (a) Ignarro, L. J. *Nitric Oxide: Biology and Pathobiology*; Academic Press: San Diego, 2000. (b) Ko, G. Y.; Fang, F. C. *Nitric Oxide and Infection*; Kluwer Academic/Plenum Publishers: New York, 1999. (c) Lincoln J.; Burnstock G. *Nitric Oxide in Health and Disease*; Cambridge University Press: New York, 1997.
(2) (a) Ying, L.; Hofseth, L. J. *Cancer Res.* **2007**, *67*, 1407–1410. (b) Li, H.; Igarashi, J.; Jamal, J.; Yang, W.; Poulos, T. L. *J. Biol. Chem.* **2006**, *11*, 753–768. (c) Rosen, G. M.; Tsai, P.; Pou, S. *Chem. Rev.* **2002**, *102*, 1191–1199. (d) Alderton, W. K.; Cooper, C. E.; Knowles, R. G. *Biochem. J.* **2001**, *357*, 593–615.
(3) (a) Hirst, D.; Robson, T. *J. Pharm. Pharmacol.* **2007**, *59*, 3–13. (b) Bonavida, B.; Khineche, S.; Huerta-Yepez, S.; Garbán, H. *Drug Res. Updates* **2006**, *9*, 157. (c) Li, C. Q.; Wogan, G. N. *Cancer Lett.* **2005**, *226*, 1–15.
(4) (a) Brüne, B. *Cell Death Differ.* **2003**, *10*, 864–869. (b) Brüne, B.; von Knethan, A.; Sandau, K. B. *Cell. Singal.* **2001**, *13*, 525–533. (c) Abramson, S. B.; Amin, A. R.; Clancy, R. M.; Attur, M. *Best Pract. Res. Clin. Rheumatol.* **2001**, *15*, 831–845.
(5) (a) Mocellin, S.; Bronte, V.; Nitti, D. *Med. Res. Rev.* **2007**, *27*, 317–352. (b) Bobba, A.; Atlante, A.; Moro, L.; Calissano, P.; Marra, E. *Apoptosis* **2007**, *12*, 1597–1610. (c) Wink, D. A.; Vodovotz, Y.; Laval, J.; Laval, F.; Dewhirst, M. W.; Mitchell, J. B. *Carcinogenesis* **1998**, *19*, 711–721. (d) Dimmeler, S.; Zeihar, A. M. *Nitric Oxide* **1997**, *1*, 275–281.
(6) (a) Tarr, J. M.; Eggleton, P.; Winyard, P. G. *Curr. Pharm. Design* **2006**, *12*, 4445–4468. (b) Payne, C. M.; Waltmire, C. N.; Crowley, C.; Crowley-Weber, C. L.; Dvorakova, K.; Bernstein, H.; Bernstein, C.; Holubec, H.; Garewal, H. *Cell Biol. Toxicol.* **2003**, *19*, 373–392. (c) Taylor, E. L.; Megson, I. L.; Haslett, C.; Rossi, A. G. *Cell Death Differ.* **2003**, *10*, 418–430. (d) Vakkala, M.; Kahlos, K.; Lakari, E.; Paakko, P.; Kinnula, V.; Soini, Y. *Clin. Cancer Res.* **2000**, *6*, 2408–2416.
(7) (a) Fukumura, D.; Kashiwagi, S.; Jain, R. K. *Nat. Rev. Cancer* **2006**, *6*, 521–534. (b) Lancaster, J. R.; Xie, K. P. *Cancer Res.* **2006**, *66*, 6459–6462. (c) Xie, K. P.; Suyun, H. *Free Radical Biol. Med.* **2003**, *34*, 969–986.

10.1021/ja801823f CCC: $40.75

donors to destroy malignant locales under controlled conditions.[12,13] Typical systemic NO donors such as organic nitrites (RONO) and nitrates ($RONO_2$), *S*-nitrosothiols (RSNO), and diazeniumdiolates (NONOates), however cannot be used for such purposes because they all slowly release NO (except specific NONOates)[14] over the course of several hours in response to ubiquitous stimuli such as heat, changes in pH, or enzymatic activity. This inexorability of systemic NO donors severely limits their use in promoting localized surges of NO, required to ensure apoptosis at tumor sites. As a consequence, precise targeting of NO to malignant tumors versus healthy tissues remains as a challenge in cancer therapy.

With the development of photodynamic therapy (PDT) as a treatment modality for certain (especially skin) cancers,[15] there has been much interest in developing light-activated NO donors.[16] Such light-triggered NO donors could provide a highly localized "burst" of NO at malignant sites under the total control of a physician's PDT laser. Among the organic NO donors, only RSNO and certain NONOates exhibit moderate photosensitivity.[16,17] However, several transition metal complexes of NO (metal nitrosyls) are known to be photoactive and release NO only when exposed to light of certain frequencies.[18] In most cases, the NO photolability arises from photoexcitation of the $d_\pi(M) \rightarrow \pi^*(NO)$ transition observed in the electronic absorption spectra of such nitrosyls. For example, the iron nitrosyl sodium nitroprusside ($Na_2[Fe(NO)(CN)_5]$, SNP) exhibits its $d_\pi(Fe) \rightarrow \pi^*(NO)$ transition in the visible region ($\lambda_{max} = 530$ nm) and releases NO under illumination with visible light.[19] Although SNP exhibits a notably high quantum yield ($\phi_{436} = 0.18$), biological studies have shown that slow release of ancillary cyanide (CN^-) ligands results in severe side effects.[20] Other iron nitrosyls like Roussin's salt esters (RSE) of the general formula $[Fe_2(\mu\text{-}SR)_2(NO)_4]$ release NO with much less efficiency ($\phi_{546} = 0.00019$),[21] while Red and Black Roussin's salts[22] are highly toxic in certain cell lines even under dark conditions.[20,23] Use of multidentate chelating ligands could provide relief to side effects arising from dissociation of monodentate ligands (such as CN^- in SNP) and, in recent years, a few heme and nonheme nitrosyls such as $[(TPP)Fe(NO)(Cl)]$[24] and $[(PaPy_3)Fe(NO)](BF_4)_2$[25] have shown considerable promise. However, these nitrosyls exhibit unpredictable stability in aqueous solution due to spontaneous $NO \rightarrow NO_2$ conversion,[26] NO_x disproportionation,[27] and fast (within ns) M−NO recombination[24] following photolysis (in case of heme).

Ruthenium nitrosyls, however, are far more stable and yet exhibit a significant degree of photolability of the bound NO.[28] For example, the $\{Ru-NO\}^6$ type of ruthenium nitrosyls such

(8) (a) Brown, G. C. *Frontiers Biosci.* **2007**, *12*, 1024–1033. (b) Szundi, I.; Rose, M. J.; Sen, I.; Eroy-Reveles, A. A.; Mascharak, P. K.; Einarsdóttir, Ó. *Photochem. Photobiol.* **2006**, *82*, 1377–1384. (c) Zhang, J.; Jin, B.; Li, L.; Block, E. R.; Patel, J. M. *Am. J. Physiol. Cell Physiol.* **2005**, *288*, C840–C849. (d) Kadenbach, B.; Arnold, S.; Lee, I.; Hüttermann, M. *Biochim. Biophys. Acta* **2004**, *1655*, 400–408.

(9) (a) Boyd, C. S.; Cadenas, E. *Biol. Chem.* **2002**, *383*, 411–423. (b) Brown, G. C. *Biochim. Biophys. Acta* **2001**, *1504*, 46–57. (c) Brüne, B.; von Knethen, A.; Sandau, K. B. *Eur. J. Pharmacol.* **1998**, *351*, 261–272.

(10) (a) Du, C.; Guan, Q.; Diao, H.; Yin, Z.; Jevnikar, A. M. *Am. J. Physiol.* **2006**, *290*, F1044–F1054. (b) Chung, P.; Cook, T.; Liu, K.; Vodovotz, Y.; Zamora, R.; Finkelstein, S.; Billiar, T.; Blumberg, D. *Nitric Oxide* **2003**, *8*, 119–126. (c) Chae, H. J.; Chae, S.-W.; An, N.-H.; Kim, J.-H.; Kim, C.-W.; Yoo, S.-K.; Kim, H.-H.; Lee, Z.-L.; Kim, H.-R. *Biol. Pharm. Bull.* **2001**, *24*, 453–460. (d) Brüne, B.; Mohr, S. *Curr. Protein Pept. Sci.* **2001**, *2*, 61–72.

(11) (a) McLaughlin, L. M.; Demple, B. *Cancer Res.* **2005**, *65*, 6097–6104. (b) Martin, L. J.; Chen, K.; Liu, Z. *J. Neurosci.* **2005**, *25*, 6449–6459. (c) Cook, T.; Wang, Z.; Alber, S.; Liu, K.; Watkins, S. C.; Vodovotz, Y.; Billiar, T. R.; Blumberg, D. *Cancer Res.* **2004**, *64*, 8015–8021. (d) Brune, B.; Schneiderhan, N. *Toxicol. Lett.* **2003**, *139*, 119–123.

(12) (a) Wang P. G.; Cai T. B.; Taniguchi N. *Nitric Oxide Donors for Pharmaceutical and Biological Applications*; Wiley-VCH: Weinheim, 2005. (b) Gasco, A.; Fruttero, R.; Rolando, B. *Rev. Med. Chem.* **2005**, *5*, 217–229. (c) Napoli, C.; Ignarro, L. J. *Annu. Rev. Pharmacol. Toxicol.* **2003**, *43*, 97–123. (d) Jia, Q. A.; Janczuk, A. J.; Cai, T. W.; Xian, M.; Wen, Z.; Wang, P. G. *Expert Opin. Ther. Pat.* **2002**, *12*, 819–826.

(13) (a) Al-Sádoni, H. H.; Ferro, A. *Rev. Med. Chem.* **2005**, *5*, 247–254. (b) Wang, P. G.; Xian, M.; Tang, X.; Wu, X.; Wen, Z.; Cai, T.; Janczuk, A. J. *Chem. Rev.* **2002**, *102*, 1091–1134. (c) Butler, A. R.; Megson, I. L. *Chem. Rev.* **2002**, *102*, 1155–1165.

(14) (a) Velazquez, C. A.; Rao, P.; Citro, M. L.; Keefer, L. K.; Knaus, E. E. *Bioorg. Med. Chem.* **2007**, *15*, 4767–4774. (b) Keefer, L. K. *Curr. Topics Med. Chem.* **2005**, *5*, 625–634. (c) Saavedra, J. E.; Shami, P. J.; Wang, L. Y.; Davies, K. M.; Booth, M. N.; Citro, M. L.; Keefer, L. K. *J. Med. Chem.* **2000**, *43*, 261–269.

(15) (a) Castano, A. P.; Mroz, P.; Hamblin, M. R. *Nat. Rev. Cancer* **2006**, *6*, 535–545. (b) Pandey, R. K. J. *Porph. Pthal.* **2006**, *4*, 368–373. (c) Detty, M. R.; Gibson, S. L.; Wagner, S. J. *J. Med. Chem.* **2004**, *47*, 3897–3915. (d) Dolmans, D. E. J. G.; Fukumora, D.; Jain, R. K. *Nat. Rev. Cancer* **2003**, *3*, 380–387.

(16) (a) Pavlos, C. M.; Xu, H.; Toscano, J. P. *Curr. Top. Med. Chem.* **2005**, *5*, 635–645. (b) Bigio, I. J.; Bown, S. G. *Cancer Biol. Therapy* **2004**, *3*, 259–267.

(17) (a) Srinivasan, A.; Kebede, N.; Saavedra, J. E.; Nikolaitchik, A. V.; Brady, D. A.; Yourd, E.; Davies, K. M.; Keefer, L. K.; Toscano, J. P. *J. Am. Chem. Soc.* **2001**, *123*, 5465–5472. (b) Zhelyaskov, V. R.; Gee, K. R.; Godwin, D. W. *Photochem. Photobiol.* **1998**, *67*, 282–288. (c) Wood, P. D.; Mutus, B.; Redmond, R. W. *Photochem. Photobiol.* **1996**, *64*, 518–524.

(18) (a) Rose, M. J.; Mascharak, P. K. *Curr. Opin. Chem. Biol.* **2008**, *12*, 238–244. (b) Ford, P. C.; Bourassa, J.; Miranda, K.; Lee, B.; Lorkovic, I.; Boggs, S.; Kudo, S.; Laverman, L. *Coord. Chem. Rev.* **1998**, *171*, 185–202. (c) Richter-Addo, G. B.; Legzdins, P. *Metal Nitrosyls*; Oxford University Press: Oxford, UK 1992.

(19) (a) Szacilowski, K.; Wacyk, W.; Stochel, G.; Stasicka, Z.; Sostero, S.; Traverso, O. *Coord. Chem. Rev.* **2000**, *208*, 277–297. (b) Stochel, G.; Wanat, A.; Kulis, E.; Stasicka, Z. *Coord. Chem. Rev.* **1998**, *171*, 203–220. (c) Singh, R. J.; Hogg, N.; Neese, F.; Joseph, J.; Kalyanaraman, B. *Photochem. Photobiol.* **1995**, *61*, 325–330. (d) Wolfe, S. K.; Swinehart, J. H. *Inorg. Chem.* **1975**, *14*, 1049–1053.

(20) (a) Alaniz, C.; Watts, B. *Ann. Pharmacother.* **2005**, *39*, 388–389. (b) Ryu, J.-S.; Lloyd, D. *FEMS Microbiol. Letts.* **1995**, *130*, 183–188.

(21) Conrado, C.; Bourassa, J. L.; Egler, C.; Wecksler, S.; Ford, P. C. *Inorg. Chem.* **2003**, *42*, 2288–2293.

(22) (a) Bourassa, J. L.; Ford, P. C. *Coord. Chem. Rev.* **2000**, *200−202*, 887–900. (b) Bourassa, J.; Lee, B.; Bernard, S.; Schoonover, J.; Ford, P. C. *Inorg. Chem.* **1999**, *38*, 2947–2952.

(23) (a) Janczyk, A.; Wolnicka-Glubisz, A.; Chmura, A.; Elas, M.; Matuszak, Z.; Stochel, G.; Urbanska, K. *Nitric Oxide* **2004**, *10*, 42–50. (b) Bourassa, J.; DeGraff, W.; Kudo, S.; Wink, D. A.; Mitchell, J. B.; Ford, P. C. *J. Am. Chem. Soc.* **1997**, *119*, 2853–2860.

(24) (a) Lim, M. D.; Lorkovic, I. M.; Wedeking, K.; Zanella, A. W.; Works, C. F.; Massick, S. M.; Ford, P. C. *J. Am. Chem. Soc.* **2002**, *124*, 9737–9743. (b) Hoshino, M.; Laverman, L.; Ford, P. C. *Coord. Chem. Rev.* **1999**, *187*, 75–102.

(25) (a) Patra, A. K.; Rowland, J. M.; Marlin, D. S.; Bill, E.; Olmstead, M. M.; Mascharak, P. K. *Inorg. Chem.* **2003**, *42*, 6812–6823. (b) Patra, A. K.; Afshar, R. K.; Olmstead, M. M.; Mascharak, P. K. *Angew. Chem., Intl. Ed.* **2002**, *41*, 2512–2515.

(26) (a) Afshar, R. K.; Eroy-Reveles, A. A.; Olmstead, M. M.; Mascharak, P. K. *Inorg. Chem.* **2006**, *45*, 10347–10354. (b) Patra, A. K.; Afshar, R. K.; Rowland, J. M.; Olmstead, M. M.; Mascharak, P. K. *Angew. Chem., Int. Ed.* **2003**, *42*, 4517–4521. (c) Ford, P. C.; Lorkovic, I. M. *Chem. Rev.* **2002**, *102*, 993–1018. (d) Bottomley, F. *Acc. Chem. Res.* **1978**, *11*, 158–163.

(27) (a) Patra, A. K.; Rose, M. J.; Olmstead, M. M.; Mascharak, P. K. *J. Am. Chem. Soc.* **2004**, *126*, 4780–4781. (b) Lim, M. D.; Lorkovic, I. M.; Ford, P. C. *Inorg. Chem.* **2002**, *41*, 1026–1028. (c) Lin, R.; Farmer, P. J. *J. Am. Chem. Soc.* **2001**, *123*, 1143–1150. (d) Lorkovic, I. M.; Ford, P. C. *Inorg. Chem.* **1999**, *38*, 1467–1473. (e) Franz, K. J.; Lippard, S. J. *J. Am. Chem. Soc.* **1998**, *120*, 9034–9040.

(28) Rose, M. J.; Mascharak, P. K. *Coord. Chem. Rev.* **2008**, . in press, doi:10.1016/j.ccr.2007.11.011.

as $K_2[Ru(NO)(Cl)_5]$[29] or $[Ru(NH_3)_5(NO)](PF_6)_3$[30] are known to release NO upon UV irradiation. Since these nitrosyls display their $d_\pi(Ru) \rightarrow \pi^*(NO)$ transitions in the UV region (300−400 nm), they can only be activated to deliver NO by UV light. Current PDT treatments, however, require photoactivation of the drug by visible light mostly to avoid the harmful effects of UV light on biological tissues. It is therefore evident that a new approach to sensitize ruthenium nitrosyls to visible light is required for their successful use in PDT.

We have recently devised a two-stage synthetic strategy to isolate ruthenium nitrosyls that exhibit significant photosensitivity under visible light. In the first stage, we employ a tetradentate dicarboxamide N_4 ligand frame, namely H_2bpb (where H_2bpb = *N*,*N*′-bis(pyridine-2-carboxamido)-1,2-diaminobenzene; H = dissociable carboxamide protons) that can be altered as required.[31,32] Rational substitutions on this ligand frame have afforded a series of ruthenium nitrosyls of the type $[(R_2byb)Ru(NO)(L)]$ (R = H, Me, OMe; *y* = p (pyridine), Q (quinoline); $L = Cl^-$, py, OH^-).[31] In this series of $\{Ru-NO\}^6$ nitrosyls, we have been able to systematically move the absorption maximum (λ_{max}) of the $d_\pi(Ru) \rightarrow \pi^*(NO)$ transition (photoband)[33] to longer wavelengths. The strategy has been very effective in moving the photoband of the resulting $\{Ru-NO\}^6$ nitrosyl from 390 nm (in case of [(bpb)Ru(NO)(Cl)]) to 500 nm (in case of [((OMe)$_2$bQb)Ru(NO)(Cl)]). The planar tetradentate ligand frame of these photosensitive nitrosyls also allows the binding of an exogenous ligand (trans to NO) via simple replacement of the chloride ligand.

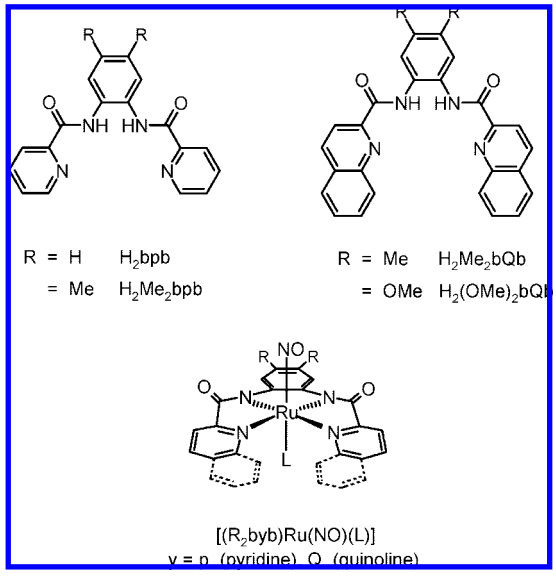

As part of the second stage of this synthetic approach, we have now enhanced the photosensitivity of these designed nitrosyls further by *directly coordinating* a light harvesting chromophore to the ruthenium center. The dye molecule Resorufin (Resf = 7-hydroxy-3H-phenoxazin-3-one)[34] has been chosen as the sensitizer because it exhibits strong absorbance in the visible region ($\lambda_{max} \approx 600$ nm, $\epsilon = 105\,000\ M^{-1}\ cm^{-1}$). In this work, we report the syntheses, structures, and properties of three such nitrosyl-dye conjugates, namely, [(Me$_2$bpb)Ru(NO)(Resf)] (**1-Resf**),[35] [(Me$_2$bQb)Ru(NO)(Resf)] (**2-Resf**), [((OMe)$_2$bQb)Ru(NO)(Resf)] (**3-Resf**). The various parameters of NO photolability of these conjugates, as reported in this account, clearly indicate that the combined strategy of ligand design and direct attachment of a dye chromophore indeed affords *ruthenium nitrosyls that are sensitive to visible light*. This strategy provides superior sensitization of metal nitrosyls compared to the pendant chromophore approach of Ford and co-workers, where the chromophore is not directly bonded to the metal center.[36] Additionally, we have employed these nitrosyl-dye conjugates to deliver NO to MDA-MB-231 breast cancer cells and promote NO-induced apoptosis. The fluorescence properties of these conjugates can be exploited in their use as "trackable" NO donors in such NO delivery. Results of the latter studies, as reported in this paper, clearly attest their utility as PDT photochemotherapeutics. The structure and photochemistry of **1-Resf** was reported in our previous communication.[35]

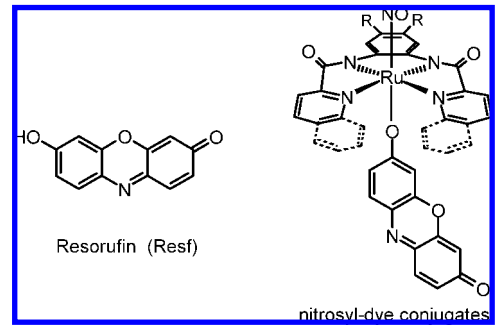

Experimental Section

Materials and General Procedures. Quinaldic acid, picolinic acid, $P(OPh)_3$, *o*-phenylenediamine, and Resorufin (as Na salt) were obtained from Sigma-Aldrich Chemical Co, whereas *O*-methylated resorufin was purchased from Fluka. $AgBF_4$ and 1,2-dimethoxy-4,5-dinitrobenzene were procured from Alfa-Aesar. The ligands H_2Me_2bpb and H_2Me_2bQb were synthesized according to the published procedures.[31] Commercially available $RuCl_3 \bullet xH_2O$ (Sigma) was used to prepare $RuCl_3 \bullet 3H_2O$. NO gas was purchased from Spectra Gases, Inc. and purified as previously described.[35] Solvents were purchased from Fisher Scientific, and distilled according to standard procedures: Et_2O, THF, and toluene from Na; CH_2Cl_2 and MeCN from CaH_2; $CHCl_3$ from K_2CO_3; pyridine from KOH; DMF from BaO; pentane was used without further purification. The starting complexes [(Me$_2$bpb)Ru(NO)(Cl)] and [(Me$_2$bQb)Ru(NO)(Cl)] were synthesized by following procedures reported by us previously.[31]

Syntheses of Metal Complexes. [(Me$_2$bpb)Ru(NO)(Resf)] (1-Resf). A batch of 0.200 g (0.391 mmol) of [(Me$_2$bpb)Ru(NO)(Cl)] was slurried in 20 mL of MeCN and treated with $AgBF_4$

(29) (a) Nikol'skii, A. B.; Popov, A. M.; Vasilevskii, I. V. *Koord. Khimiya.* **1976**, *2*, 671–677. (b) Cox, A. B.; Wallace, R. M. *Inorg. Nucl. Chem. Letts.* **1971**, *7*, 1191–1194.
(30) Toledo, J. C.; Ledo, B. D. S. L.; Franco, D. W. *Coord. Chem. Rev.* **2005**, *249*, 419–431.
(31) Patra, A. K.; Rose, M. J.; Murphy, K. M.; Olmstead, M. M.; Mascharak, P. K. *Inorg. Chem.* **2004**, *43*, 4487–4495.
(32) (a) Afshar, R. K.; Eroy-Reveles, A. A.; Olmstead, M. M.; Mascharak, P. K. *Inorg. Chem.* **2006**, *45*, 10347–10354. (b) Patra, A. K.; Rose, M. J.; Olmstead, M. M.; Mascharak, P. K. *J. Am. Chem. Soc.* **2004**, *126*, 4780–4781.
(33) (a) Sizova, O. V.; Lyubimova, O. O. *Russ. J. Gen. Chem.* **2004**, *74*, 996–1000. (b) Greene, S. N.; Richards, N. G. J. *Inorg. Chem.* **2004**, *43*, 7030–7041.
(34) (a) Zollinger, H. *Color Chemistry: Syntheses, Properties, and Applications of Organic Dyes and Pigments, 3rd Ed.*; Wiley-VCH and Verlag Helvetica Chimica Acta: Zurich, Switzerland, 2003. (b) Griffith, J. Ed. *Developments in the Chemistry and Technology of Organic Dyes*; Blackwell Scientific: Oxford, 1984.
(35) Rose, M. J.; Olmstead, M. M.; Mascharak, P. K. *J. Am. Chem. Soc.* **2007**, *129*, 5342–5343.
(36) Ford, P. C.; Wecksler, S. *Coord. Chem. Rev.* **2005**, *249*, 1382–1395.

(0.076 g, 0.391 mmol) dissolved in 5 mL of MeCN. This mixture was heated to reflux for 12 h to generate a turbid brown-green solution, which was cooled to room temperature and filtered through a Celite pad to remove AgCl. One equiv (0.101 g, 0.391 mmol) of Resorufin dye (as Na salt) was then added, and the reaction mixture was heated for another 16 h to generate a bright red solution. This solution was cooled to −20 °C overnight and filtered to remove trace amount of excess dye. The filtrate was then concentrated to one-third volume and again placed at −20 °C to afford **1-Resf** as a bright red solid. Yield: 117 mg (56%). Anal. Calcd. for $C_{32}H_{22}N_6O_6Ru$ (**1**): C 55.89, H 3.22, N 12.22; Found: C 56.03, H 3.28, N 12.14. X-ray quality crystals of **1-Resf**•H_2O were obtained by $CHCl_3$/pentane vapor diffusion at 35 °C. Selected IR frequencies (KBr disk, in cm^{-1}): 1841 (vs ν_{NO}), 1632 (vs ν_{CO}), 1595 (vs), 1484 (s), 1367 (m), 1276 (s ν_{ArCO}), 1206 (w), 1097 (w), 864 (w), 759 (w), 685 (w). UV/vis in MeCN, λ in nm (ϵ in M^{-1} cm^{-1}): 280 (11 860), 310 sh (6 680), 395 sh (6 000), 500 (11 920). ^{1}H NMR in $CDCl_3$, δ from TMS: 8.81 (d 2H), 8.39 (s 2H), 8.35 (d 2H), 8.25 (t 2H), 7.77 (t 2H), 7.30 (d 2H), 7.12 (d 2H), 6.74 (d 1H), 6.15 (s 1H), 5.93 (d 1H), 5.62 (d 1H), 2.93 (s 6H).

[(Me_2bpb)Ru(NO)(OH)] (1-OH). A batch of [(Me_2bpb)Ru(NO)(Cl)] (0.200 g, 0.391 mmol) was treated with 1 equiv of $AgBF_4$ (0.039 g, 0.200 mmol) in MeCN under reflux conditions as described above. Following filtration, several drops of water and 3 equiv of aniline (0.109 g, 1.17 mmol) were added as base. Upon further heating for 16 h, the solution turned pale orange. It was then concentrated to 5 mL and stirred at room temperature for several h when **1-OH** precipitated out as an orange solid. Yield: 105 mg (55%). Anal. Cacld. for $C_{20}H_{17}N_5O_4Ru$ (**1-OH**): C 48.78, H 3.48, N 14.22; Found: C 48.52, H 3.55, N 13.93. X-ray quality crystals of **1-OH**•DMSO were grown by vapor diffusion of acetone into a biphasic DMSO/Et_2O mixture of **1-OH** at ambient temperature. Selected IR frequencies (KBr disk, in cm^{-1}): 1828 (s ν_{NO}), 1621 (s ν_{CO}), 1587 (vs), 1564 (m), 1483 (m), 1388 (m), 1097 (w), 1008 (w), 758 (m), 685 (m), 485 (w). UV/vis in DMF, λ in nm (ϵ in M^{-1} cm^{-1}): 305 (7 020), 390 (5 100). ^{1}H NMR in DMSO, δ from TMS: 9.13 (d 2H), 8.34 (m 2H), 8.32 (s 2H) 8.13 (d 2H), 7.85 (m 2H), 3.34 (s 6H).

[(Me_2bQb)Ru(NO)(Resf)] (2-Resf). One equiv of $AgBF_4$ (0.032 g, 0.165 mmol) was added to a slurry of [(Me_2bQb)Ru(NO)(Cl)] (0.100 g, 0.165 mmol) in MeCN (20 mL) and the mixture was heated to reflux for 16 h when a turbid brown solution was obtained. It was filtered through Celite to remove AgCl. Next, 1 equiv of Resorufin (as Na salt, 0.040 g, 0.166 mmol) was added and the slurry was heated at reflux for an additional 24 h. The bright red solution thus obtained was cooled to room temperature, filtered, and concentrated to 10 mL. It was then stored at −20 °C. Dark red microcrystals of **2-Resf** precipitated from the solution within 72 h which were isolated by filtration, washed with small portions of Et_2O and dried. Yield: 40 mg (44%). Anal. Calcd. for $C_{40}H_{26}N_6O_6Ru$ (**3**): C 60.99, H 3.33, N 10.67; Found: C 60.72, H 3.48, N 10.89. X-ray quality crystals of **2-Resf**•$CHCl_3$ were grown via $CHCl_3$/pentane vapor diffusion at 35 °C. Selected IR frequencies (KBr disk, in cm^{-1}): 1847 (s ν_{NO}), 1631 (vs ν_{CO}), 1585 (s), 1558 (m), 1485 (m), 1368 (m), 1281 (s ν_{ArCO}), 798 (w), 462 (w). UV/vis in MeCN, λ in nm (ϵ in M^{-1} cm^{-1}): 300 (16 900), 510 (12 300). ^{1}H NMR in $CDCl_3$, δ from TMS: 8.74 (d 2H), 8.54 (d 2H), 8.37 (s 2H), 8.14 (d 4H), 7.80 (t 2H), 7.55 (t 2H), 7.35 (m 1H), 7.10 (d 1H), 6.72 (d 1H), 6.09 (s 1H), 6.03 (d 1H), 5.69 (s 1H).

[(Me_2bQb)Ru(NO)(OH)] (2-OH). The starting complex [(Me_2bQb)Ru(NO)(Cl)] (150 mg, 0.26 mmol) and 1 equiv of $AgBF_4$ (50 mg, 0.26 mmol) were dissolved in 15 mL of DMF and the solution was heated to reflux for 3 h. It was then cooled and AgCl was filtered off using a Celite pad. To the filtrate was added 3 equiv of aniline (72 mg, 0.78 mmol) and several drops of water. The solution was again heated to reflux for 3 h. Next, the solvent was removed in vacuo and the residue was triturated several times with MeCN. Finally, the residue was stirred in 5 mL of MeCN for 30 min and the red product (**2-OH**) was isolated by filtration. Yield: 66 mg (45%). Anal. Calcd. for $C_{28}H_{21}N_5O_4Ru$ (**2-OH**): C 56.56, H 3.90, N 11.78; Found: C 56.30, H 3.88, N 11.89. Selected IR bands (KBr disk, in cm^{-1}): 1837 (s ν_{NO}), 1632 (vs ν_{CO}), 1594 (m), 1561 (w), 1511 (w), 1483 (w), 1456 (w), 1372 (m), 1341 (w), 1007 (w), 760 (w), 726 (m). UV/vis in DMF, λ in nm (ϵ in M^{-1} cm^{-1}): 310 (16 080), 445 (3 150). ^{1}H NMR in $CDCl_3$, δ from TMS: 8.69 (d 2H), 8.56 (d 2H), 8.42 (s 2H), 8.06 (d 2H), 7.93 (d 2H), 7.71 (t 2H), 7.43 (t 2H), 2.34 (s 6H).

H_2($OMe)_2$bQb. A mixture of 1,2-dimethoxy-4,5-diaminobenzene[37] (0.51 g, 3.0 mmol), 2 equiv of quinaldic acid (1.04 g, 6.0 mmol) and 2 equiv of $P(OPh)_3$ (1.87 g, 6.0 mmol) were dissolved in 20 mL of pyridine. The greenish-brown solution turned red upon heating at 100 °C for 3 h. The solution was cooled and kept at 4 °C for several days. The resulting yellow precipitate was filtered and washed several times with EtOH. Yield: 1.04 g (72%). Selected IR bands (KBr disk, in cm^{-1}): 1677 (s ν_{CO}), 1611 (w), 1533 (vs), 1480 (s), 1426 (m), 1355 (m), 1213 (s), 1114 (w), 1083 (m), 844 (m), 772 (s), 562 (w). ^{1}H NMR in $CDCl_3$, δ from TMS: 10.49 (s 2H), 8.47 (d 2H), 8.39 (d 2H), 7.91 (t 2H), 7.86 (t 2H), 7.64 (s 2H), 7.62 (m 4H), 3.99 (s 6H).

[(($OMe)_2$bQb)Ru(NO)(Cl)] (3-Cl). A yellow solution of $H_2(OMe)_2$bQb (0.100 g, 0.21 mmol) in 10 mL of DMF was treated with 2.2 equiv of NaH (11 mg, 0.46 mmol) to generate a bright pink solution. Separately, $RuCl_3$•$3H_2O$ (55 mg, 0.21 mmol) was dissolved in 2 mL of DMF and added to the solution of the deprotonated ligand. The green mixture was then heated to reflux for 16 h. Next, it was cooled to room temperature and filtered to remove NaCl. The dark green filtrate was degassed and NO gas was bubbled through it at reflux temperature for 1 h. The resulting red solution was cooled, and the solvent was removed in vacuo. The oily residue was triturated several times with MeCN to afford a brown solid. This solid was then washed with several portions of MeCN (2 × 5 mL) and THF (2 × 5 mL), and the brown filtrates were discarded. The dark red product (**3-Cl**) thus obtained was finally dried in vacuo. Yield: 54 mg (40%). Anal. Calcd. for $C_{28}H_{20}ClN_5O_5Ru$ (**3-Cl**): C 52.14, H 3.44, N 10.86; Found: C 52.32, H 3.48, N 10.89. Selected IR bands (KBr disk, in cm^{-1}): 1829 (vs, ν_{NO}), 1623 (vs, ν_{CO}), 1593 (m), 1560 (w), 1512 (m), 1498 (s), 1458 (m), 1402 (m), 1373 (m), 1282 (w), 1216 (m), 1081 (m), 997 (w), 871 (w), 761 (m), 458 (w). UV/vis in DMF, λ in nm (ϵ in M^{-1} cm^{-1}): 320 (21 530), 490 (3 750). ^{1}H NMR in $CDCl_3$, δ from TMS: 8.68 (d 2H), 8.53 (d 2H), 8.49 (s 2H), 8.07 (d 2H), 8.04 (d 2H), 7.74 (t 2H), 7.48 (t 2H), 4.02 (s 6H).

[(($OMe)_2$bQb)Ru(NO)(OH)] (3-OH). This nitrosyl was synthesized in 40% yield by following the procedure used for isolating **2-OH**. Anal. Calcd. for $C_{28}H_{21}N_5O_6Ru$ (**3-OH**): C 53.67, H 3.70, N 11.18; Found: C 53.72, H 3.48, N 11.09. Selected IR bands (KBr disk, cm^{-1}): 1852 (s, ν_{NO}), 1625 (vs, ν_{CO}), 1591 (w), 1498 (s), 1401 (m), 1215 (m), 1078 (w), 762 (m). UV/vis in DMF, λ in nm (ϵ in M^{-1} cm^{-1}): 320 (25 200), 490 (4 030).

[(($OMe)_2$bQb)Ru(NO)(Resf)] (3-Resf). A mixture of **3-Cl** (0.100 g, 0.16 mmol) and 1 equiv of $AgBF_4$ (30 mg, 0.16 mmol) in 35 mL of MeCN was heated to reflux for 3 h. It was then filtered to remove AgCl. The dark red filtrate was heated to reflux and to the hot solution was added a batch of 37 mg (0.16 mmol) of Resorufin (sodium salt). After 4 h of heating, the solution was cooled and filtered to remove trace amount of unreacted dye. The solvent was then evaporated and the residue was extracted with 10 mL of $CHCl_3$. The dark red $CHCl_3$ solution was loaded on a silica gel column. Next, the column was eluted with CH_2Cl_2 with increasing amounts (10−100%) of THF. The bright red fraction which eluted with 50% THF was collected. Vapor diffusion of Et_2O into this solution over several days afforded dark red crystals of **3-Resf**. Anal. Calcd. for $C_{40}H_{26}N_6O_8Ru$ (**3-Resf**): C 60.07, H 3.69, N 10.25; Found: C 60.12, H 3.49, N 10.29. Yield: 20 mg (15%). Selected IR bands (KBr disk, in cm^{-1}): 1848 (vs, ν_{NO}), 1623 (vs, ν_{CO}), 1584 (vs), 1560 (s), 1490 (vs), 1440 (m), 1400 (m), 1362

(37) Rosa, D. T.; Reynolds, R. A.; Malinak, S. M.; Coucouvanis, D. *Inorg. Synth.* **2002**, *33*, 112–119.

Table 1. Summary of Crystal Data, Intensity Collection and Refinement Parameters for [(Me_2bpb)Ru(NO)(Resf)]•H_2O (**1-Resf**•H_2O), [(Me_2bQb)Ru(NO)(Resf)]•$CHCl_3$ (**2-Resf**•$CHCl_3$), and [(($OMe)_2$bQb)Ru(NO)(Resf)] (**3-Resf**)

	1-Resf	2-Resf	3-Resf
empirical formula	$C_{32}H_{24}N_6O_7Ru$	$C_{41}H_{27}Cl_3N_6O_6Ru$	$C_{40}H_{26}N_6O_8Ru$
Fw	705.64	907.11	819.74
crystal color	red needle	red/purple plate	red plate
crystal size (mm)	0.22 × 0.08 × 0.07	0.25 × 0.15 × 0.07	0.13 × 0.11 × 0.02
T (K)	90(2)	153(2)	150(2)
wavelength (Å)	0.7103	0.7103	0.7749
crystal system	triclinic	monoclinic	monoclinic
space group	$P\bar{1}$	$P2_1$/n	$P2_1$/c
a (Å)	10.0845(5)	12.3639(14)	12.149(2)
b (Å)	10.7797(6)	17.278(2)	16.232(3)
c (Å)	15.0195(8)	18.019(2)	17.971(4)
α (deg)	76.0570(10)	90	90
β (deg)	71.3960(10)	113.317(1)	108.15(3)
γ (deg)	69.1370(10)	90	90
V (Å^3)	1430.94(13)	3534.9(7)	3367.6(12)
Z	2	4	4
d_{calc} (g/cm^3)	1.638	1.704	1.617
μ (mm^{-1})	0.611	0.733	0.661
GOF[a] on F^2	0.954	1.035	1.021
final R indices	$R1 = 0.0348$	$R1 = 0.0874$	$R1 = 0.0355$
[$I > 2\sigma(I)$]	w$R2 = 0.0775$	w$R2 = 0.2631$	w$R2 = 0.0900$
R indices[b]	$R1 = 0.0499$	$R1 = 0.1072$	$R1 = 0.0442$
all data[c]	w$R2 = 0.0839$	w$R2 = 0.2811$	w$R2 = 0.0955$

[a] GOF = $[\Sigma[w(F_o^2 - F_c^2)^2]/M - N)]^{1/2}$ (M = number of reflections, N = number of parameters refined). [b] $R1 = \Sigma||F_0| - |F_0||/\Sigma|F_0|$. [c] w$R2 = [\Sigma[w(F_0^2 - F_c^2)^2]/\Sigma[w(F_o^2)^2]]^{1/2}$.

Table 2. Selected Bond Distances (Å) and Angles (deg) of **1-Resf**, **2-Resf**, and **3-Resf**

	1-Resf	2-Resf	3-Resf
bond distances			
Ru−N5	1.7347(16)	1.729(7)	1.7425(19)
N5−O3	1.159(2)	1.168(8)	1.154(2)
Ru−N1	2.1250(15)	2.160(7)	2.1516(18)
Ru−N2	1.9862(15)	1.972(7)	1.9840(19)
Ru−N3	1.9803(15)	2.004(6)	1.9943(18)
Ru−N4	2.1384(15)	2.184(7)	2.1457(19)
Ru−O(Resf)	2.0110(13)	1.987(5)	1.9915(16)
O_{ph}−C(Resf)	1.328(2)	1.338(9)	1.323(3)
O_{ket}−C(Resf)	1.246(2)	1.246(12)	1.232(3)
bond angles			
Ru−N5−O3	178.13(15)	171.6(7)	174.48(19)
Ru−O−C(Resf)	128.46(11)	130.4(5)	131.80(14)

(m), 1323 (m), 1282 (s), 1214 (m), 1096 (m), 996 (w), 853 (m), 771 (m), 596 (w), 501 (w). UV/vis in MeCN, λ in nm (ϵ in M^{-1} cm^{-1}): 317 (26 000), 490 (27 900). ^{1}H NMR in $CDCl_3$, δ from TMS: 8.75 (d 2H), 8.52 (d 2H), 8.32 (s 2H), 8.13 (t 2H), 7.81 (t 2H), 7.56 (t 2H), 7.30 (d 1H), 7.12 (2 1H), 6.72 (d 1H), 6.11 (s 1H), 6.08 (d 1H), 5.67 (s 1H), 4.00 (s 6H).

X-ray Diffraction, Data Collection and Structure Solution. Diffraction data for **1-Resf**·H_2O (90 K), **1-OH**·DMSO (90 K), and **2-Resf**·$CHCl_3$ (153 K) were collected on a Bruker Apex-II diffractometer with Mo Kα radiation (λ = 0.71073 Å). The data for **3-Resf** (150 K) was obtained using synchrotron radiation (λ = 0.77490 Å) at the Lawrence-Berkeley Advanced Light Source (ALS). The structures were solved using the SHELXTL software package. An absorption correction was applied. Crystal properties, diffraction data, and parameters of the structure solution are listed in Table 1, whereas selected bond distances (Å) and bond angles (deg) are included in Table 2. The structure (Figure S1) and metric parameters of **1-OH** are included in the Supporting Information.

Physical Measurements. A Perkin-Elmer Spectrum One FTIR spectrometer was used to record the IR spectra. ^{1}H NMR spectra of the nitrosyls were obtained with a Varian 500 MHz spectrometer. Electronic absorption spectra were monitored on a Varian Cary 50 spectrophotometer. Fluorescence spectra were recorded with a Perkin-Elmer LS50B Fluorescence/Luminescence Spectrometer. Release of NO in aqueous solution upon illumination was monitored using the *in*NO Nitric Oxide Monitoring System (Innovative Instruments, Inc.) fitted with the *ami*-NO 2008 electrode. The NO amperograms were recorded using stirred solutions contained in open vials. X-band EPR spectra following photolyses were obtained using a Bruker 500 ELEXSYS spectrometer at 125 K.

Photolysis Experiments. The quantum yields of NO photorelease were obtained using a tunable Apex Illuminator (150 W xenon lamp) equipped with a Cornerstone 130 1/8 M monochromator (measured intensity of ∼10 mW). Samples were prepared in 4 × 10 mm quartz cuvettes and placed 2 cm from the light source. Actinochrome N (475/610) was used as the actinometer in the visible range.[38] Solutions were prepared at ∼0.2 mM to ensure sufficient absorbance (>90%) at the irradiation wavelength, and changes in electronic spectrum in the 750 nm region (<10% photolysis) were used to determine NO photorelease. For qualitative photolysis experiments (such as EPR and cell-based experiments), an IL 410 Illumination System from Electro-FiberOptics Corp. (halogen lamp) was used. This system was equipped with a $\lambda \geq$ 465 nm cutoff filter (measured intensity = 300 mW) to isolate visible light. The rates of NO release from the nitrosyls were measured using ∼0.05 mM solutions of the complexes in a 4 × 10 mm cuvette. The apparent rates of NO loss (k_{NO}) were monitored at an appropriate wavelength for each complex, and the k_{NO} values derived from the two parameter exponential equation $y = a*(1-\exp(-k*x))$ as provided in SigmaPlot 8.0.

Cell Culture and Fluorescence Microscopy. MDA-MB-231 breast carcinoma cells were a kind gift from Dr. Mina Bissell, and passaged in DMEM high glucose (Gibco) supplemented with 5% FBS (Gemini Bioproducts) and penicillin/streptomycin (Gibco). Cells were grown to ∼70% confluence in 8-well microscope chamber slides (Nunc Laboratory-Tek). All PBS solutions used in fluorescence experiments were supplemented with 1 mM $CaCl_2$ and 0.5 mM $MgCl_2$ (PBS-Ca/Mg). For each well, 8 μL of 5 mM stock solution of Ru−NO complex in MeCN was diluted with 192 μL of PBS-Ca/Mg. After 1 h incubation at 37 °C, cells were washed 3 times with PBS-Ca/Mg, and then exposed to 1 min of visible light ($\lambda \geq$ 465 nm, ∼0.3 W measured intensity) or kept in the dark

(38) (a) Schmidt, R.; Brauer, H.-D. *J. Photochem.* **1984**, *25*, 489–499. (b) Murov, S. *Handbook of Photochemistry*; Marcel Dekker: New York, 1973.

(control). Media was then replenished and cells incubated for various times (1−8 h) at 37 °C under 5% CO_2 atmosphere. For imaging, each well was washed 3× with PBS-Ca/Mg and fixed with 4% paraformaldehyde (PFA) for 20 min at room temperature. The fluorescein-based TUNEL assay (Roche Applied Science) was used on permeabilized cells (0.1% Triton X-100, 0.1% sodium citrate) according to manufacturer's instructions. Finally, all samples were stained with 10 μM DAPI for 15 min to visualize nuclei, washed 2× with PBS-Ca/Mg, and once with H_2O. The slides were mounted with Fluoromount-G (Southern Biotech) under glass coverslips (Fisher), and sealed with nail varnish. Fluorescence images were obtained using an Axiovert 200 fluorescence microscope (Zeiss) coupled to an AttoArc 2 HBO 100 W light source (Zeiss), equipped with a CCD camera plus SPOT Advanced software v4.0.9 (Diagnostic Instruments, Inc.). Exposure times were chosen to best reflect the image as observed through microscope lens, as follows for each color: blue (DAPI): 500 ms to 2 s; red (**1-Resf**): 5−10 s; green (TUNEL): 3−7 s (5 s minimum for darker control images).

Results and Discussion

The photosensitive nitrosyl-dye conjugates, **1-Resf**, **2-Resf**, and **3-Resf**, are derived from designed dianionic tetradentate ligands of the type R_2byb^{2-} with two carboxamido nitrogens as donors. In addition, the ruthenium centers are coordinated to the dye molecule resorufin (Resf), trans to NO. They have been synthesized from the corresponding $\{Ru-NO\}^6$ species $[(R_2byb)Ru(NO)(Cl)]$ via replacement of the chloride ligand with the anionic resorufin dye. Reaction of the chloro complexes with $AgBF_4$ in MeCN results in the formation of the MeCN-bound intermediates which afford the final nitrosyl-dye conjugates upon reaction with the sodium salt of the dye.[34] All three nitrosyl-dye conjugates are dark red solids which are thermally stable and dissolve in MeCN, DMF, DMSO, and water. Such solutions are stable when stored in the dark. Exposure to light (visible or UV) results in rapid release of NO (vide infra).

The reason for the choice of ligands in the syntheses of the photosensitive Ru−NO unit in the present complexes must be mentioned at this point. Results of our previous work have established that ligands with carboxamido nitrogen(s) as donor(s) stabilize higher oxidation states of transition metals. As a consequence, excitation of the $d_\pi(M) \rightarrow \pi^*(NO)$ transition of the $\{Ru-NO\}^6$ nitrosyls derived from such ligands leads to rapid release of NO and generation of Ru(III) photoproducts in various solvents including water (eq 1).[31,35,39–41] Quite in contrast, similar $\{Ru-NO\}^6$ nitrosyls derived from neutral pyridine-based ligands (such as bpy) and Schiff bases afford Ru(II) photoproducts following NO photorelease.[39,42] In addition, they are quite unstable in aqueous media and are readily converted to the corresponding nitro complexes due to nucleophilic attack of water to the formally NO^+ moiety of the nitrosyls.[43] The strong σ-donating negatively charged carboxamido nitrogens in the former class of nitrosyls prevent

$$(L)Ru-(NO)_{bound} + h\nu + solv \rightarrow (L)Ru(III) - solv + NO \quad (1)$$

electron transfer from the bound NO ligand to the metal centers. This is evidenced by the lower N−O stretching (ν_{NO}) frequencies (1830 − 1890 cm^{-1}) of such nitrosyls[31,35,39] compared to those values observed with neutral nitrogen donors (ν_{NO} > 1900 cm^{-1}).[42,43] As a consequence, the $\{Ru-NO\}^6$ nitrosyls derived from ligands with carboxamide groups are stable in water and exhibit greater NO photolability. The bpb-based ligand frame can also accommodate various substitutions that red shift the photoband of the resulting nitrosyls. This was necessary for our strategy since we aimed to bring the photoband close to the absorption maximum (λ_{max}) of the light-harvesting unit. Our results now demonstrate that while [(bpb)Ru(NO)(Cl)] exhibits its λ_{max} at 380 nm in MeCN, the analogous nitrosyl [((OMe)$_2$bQb)Ru(NO)(Cl)] displays its absorption band at 500 nm in the same solvent.

In the present work, we have employed the tricyclic dye resorufin (Resf), which displays intense absorption (ϵ = 105 000 M^{-1} cm^{-1}) in the visible range ($\lambda_{max} \approx$ 600 nm).[44,45] The phenolato oxygen donor of this anionic dye binds the ruthenium centers of the $[(R_2byb)Ru(NO)(solv)]$ species much like OH^- in $[(R_2byb)Ru(NO)(OH)]$.[35] Interestingly, such binding blue shifts the λ_{max} of the dye to 500 nm. This is quite an advantage since alteration of the bpb-frame of the equatorial ligand allowed us to easily merge the photoband into the absorption band of the light-harvesting unit. As discussed later, this merging greatly improves the sensitivity of the resulting nitrosyl-dye conjugates like **3-Resf** to visible light ($\lambda \geq$ 465 nm). One must note here that the present strategy is an open one; it allows use of other dyes with absorptions at longer wavelengths. The only requirement is the proper alteration(s) of the bpb-based ligand frame such that the photoband merges with the absorption band of the bound dye.

Structures. The structures of the three nitrosyl-dye conjugates have been determined in the present work to confirm the direct coordination of the resorufin dye to the ruthenium centers via the phenolato oxygen. The structure of [(Me$_2$bpb)Ru(NO)(Resf)] (**1-Resf**) was briefly reported in our earlier communication. Since alteration of the bpb-type ligand frame in these nitrosyl-dye conjugates results in significant changes in the overall structures of the final products, the structure of **1-Resf** (Figure 1) is included here for the purpose of comparison. Pertinent metric parameters of all three nitrosyl-dye conjugates are listed in Table 2.

[(Me$_2$bpb)Ru(NO)(Resf)] (1-Resf). The tetradentate dicarboxamido frame of the Me_2bpb^{2-} ligand retains its planarity to a large extent in the equatorial plane of this complex (Figure

(39) (a) Rose, M. J.; Patra, A. K.; Alcid, E. A.; Olmstead, M. M.; Mascharak, P. K. *Inorg. Chem.* **2007**, *46*, 2328–2338. (b) Patra, A. K.; Mascharak, P. K. *Inorg. Chem.* **2003**, *42*, 7363–7365.
(40) (a) Works, C. F.; Jocher, C. J.; Bart, G. D.; Bu, X.; Ford, P. C. *Inorg. Chem.* **2002**, *41*, 3728–3739. (b) Bordini, J.; Hughes, D. L.; da Motto Neto, J. D.; da Cunha, C. J. *Inorg. Chem.* **2002**, *41*, 5410–5416. (c) Works, C. F.; Ford, P. C. *J. Am. Chem. Soc.* **2000**, *122*, 7592–7593.
(41) (a) Prakash, R.; Czaja, A. U.; Heinemann, F. W.; Sellmann, D. *J. Am. Chem. Soc.* **2005**, *127*, 13758–13759. (b) Sellmann, D.; Prakash, R.; Heinemann, F. W.; Moll, M.; Klimowicz, M. *Angew. Chem., Int. Ed.* **2004**, *43*, 1877–1880.
(42) (a) Pipes, D. W.; Meyer, T. J. *Inorg. Chem.* **1984**, *23*, 2466–2472. (b) Callahan, R. W.; Meyer, T. J. *Inorg. Chem.* **1977**, *16*, 574–581.
(43) (a) de Lima, R. G.; Sauaia, M. G.; Bonaventura, D.; Tedesco, A. C. *Inorg. Chim. Acta* **2006**, *359*, 2543–2549. (b) de Lima, R. G.; Sauaia, M. G.; Bonaventura, D.; Tedesco, A. C.; Lopez, R. F. V.; Bendhack, L. M.; da Silva, R. S. *Inorg. Chim. Acta* **2005**, *358*, 2643–2650. (c) Carlos, R. M.; Cordoso, D. R.; Castellano, E. E.; Osti, R. Z.; Camargo, A. J.; Macedo, L. G.; Franco, D. W. *J. Am. Chem. Soc.* **2004**, *126*, 2546–2555. (d) Sugimori, A.; Uchida, H.; Akiyama, T.; Mukaida, M.; Shimuzu, K. *Chem. Lett.* **1982**, 1135–1138.
(44) (a) Montejano, H. A.; Gervaldo, M.; Bertolotti, S. G. *Dyes Pigments.* **2005**, *64*, 117–124. (b) Bueno, C.; Villegas, M. L.; Bertolotti, S. G.; Previtali, C. M.; Neumann, M. G.; Encinas, M. V. *Photochem. Photobiol.* **2002**, *76*, 385–390. (c) Flamigni, L.; Venuti, E.; Camaioni, N.; Barigelleti, F. *J. Chem. Soc., Faraday Trans.* **1989**, *85*, 1935–1943. (d) Fabian, J.; Hartmann, H. *Light Absorption of Organic Colorants: Theoretical Treatment and Empirical Rules*; Springer-Verlag: Heidelberg, Germany, 1980.
(45) The ε-value of unbound Resorufin (as sodium salt) was determined in DMF for the sake of comparison to the complexes described in this work.

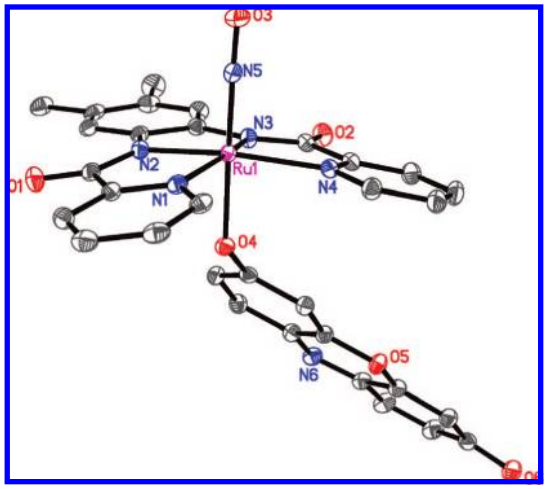

Figure 1. Thermal ellipsoid plot (shown as 50% probability ellipsoids) of [(Me_2bpb)Ru(NO)(Resf)] (**1-Resf**). H-atoms have been omitted for clarity.

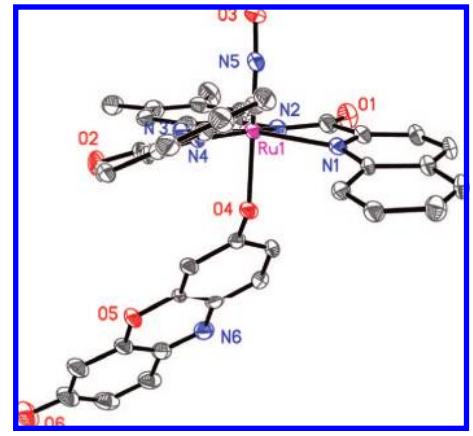

Figure 2. Thermal ellipsoid plot (shown as 30% probability ellipsoids) of [(Me_2bQb)Ru(NO)(Resf)] (**2-Resf**). H-atoms have been omitted for clarity.

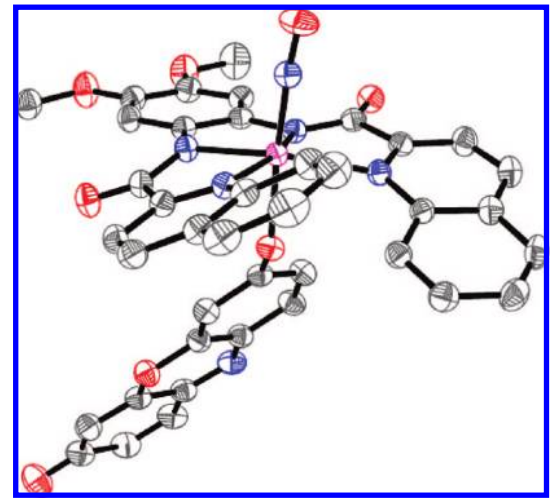

Figure 3. Thermal ellipsoid plot (shown as 50% probability ellipsoids) of [(OMe_2bQb)Ru(NO)(Resf)] (**3-Resf**). H-atoms have been omitted for clarity.

1). The ruthenium center is in pseudo-octahedral geometry with NO in one of the axial positions. The other axial position is occupied by the resorufin dye via its phenolato oxygen. The Ru−O bond distance (Ru−O4 = 2.0110(13) Å) is similar to that observed in [(salen)Ru(NO)(ONO)] (2.041(4) Å) and [($^{t\text{Bu}}$salophen)Ru(NO)(Cl)] (2.0254(13) Å).[40] The heterocyclic dye is tilted away from the equatorial plane (Ru−O4−C(Resf) = 128.46(11)°) further than expected for an sp^3 O-atom (ideally 109.5°) presumably due to steric reasons.

The Ru−NO moiety of **1-Resf** exhibits Ru−N and N−O bond distances (Ru−N5 = 1.7347(16) Å; N5−O3 = 1.159(2) Å) which are very close to those values observed with the starting species [(Me_2bpb)Ru(NO)(Cl)] (Ru−N5 = 1.742(3) Å; N5−O3 = 1.154(4) Å).[31] Also, the Ru−N−O unit is approximately linear (178.13(15)°), much like that in [(Me_2bpb)Ru(NO)(Cl)] (173.90(3)°). It is thus evident that the direct coordination of the dye to the ruthenium center of the parent nitrosyl does not affect the overall structure of the {Ru−NO}^{6} core to a significant extent.

[(Me_2bQb)Ru(NO)(Resf)] (2-Resf). Substitution of the pyridine rings of the bpb ligand frame with quinolines results in distortions in the equatorial plane of this nitrosyl-dye conjugate. As shown in Figure 2, the Me_2bQb^{2-} ligand is no longer planar. The quinoline units of the Me_2bQb^{2-} ligand frame are severely distorted due to steric hindrance arising from the extended quinoline rings. There is a net displacement of ∼35° between the two quionoline planes. As a result, the Ru−N_Q bond distances observed in **2-Resf** (Ru−N4 = 2.184(7) Å) are slightly longer than the corresponding Ru−N_{py} bond distances observed in **1-Resf** (Ru−N1 = 2.1250(15) Å). In **2-Resf**, the dye is also coordinated to the ruthenium center via its phenolato-O donor (Ru−O3 = 1.987(5) Å). However, it bends toward the dicarboxamido moiety of the ligand frame (Figure 2) even though the Ru−O3−C(Resf) angle (130.4(5)°) is similar to that observed in **1-Resf**. One must note here that the twisting of the equatorial Me_2bQb^{2-} ligand in **2-Resf** is *not* due to this reorientation of the coordinated dye unit, since the same twisting of the Me_2bQb^{2-} ligand is observed in the parent nitrosyl [(Me_2bQb)Ru(NO)(Cl)].[31] The reorientation of the dye in **2-Resf** is therefore a result of the twisted Me_2bQb^{2-} ligand in the equatorial plane.

[(($OMe)_2$bQb)Ru(NO)(Resf)] (3-Resf). The severely twisted $(OMe)_2bQb^{2-}$ ligand frame in the equatorial plane of **3-Resf** also forces the bound dye toward the dicarboxamido portion of the ligand (Figure 3). In this respect, the structures of **2-Resf** and **3-Resf** are similar. However, the Ru−N(O) bond of **3-Resf** (Ru−N5 = 1.7425(19) Å) is noticeably longer than that of **2-Resf** (1.729(7) Å). This difference most possibly arises from greater electron-donating capacity of the −OMe groups in **3-Resf** compared to the –Me groups in **2-Resf**.

Electronic Absorption Spectra. {Ru−NO}^{6} nitrosyls of the type [(bpb)Ru(NO)(Cl)] and [(Me_2bpb)Ru(NO)(Cl)] exihibit a moderately strong ($\epsilon \approx 5\,000\ M^{-1}\ cm^{-1}$) absorption band with λ_{max} in the range of 380−400 nm in solvents like MeCN and DMF.[31] Schiff base complexes, such as [(salen)Ru(NO)(Cl)], also display their absorption maxima at around 400 nm.[40]The typical orange color of these nitrosyls does not change much upon exchange of the Cl^- ligand with OH^-. For example, [(Me_2bpb)Ru(NO)(OH)] (**1-OH**) exhibits an absorption band with λ_{max} = 390 nm ($\epsilon = 5\,100\ M^{-1}\ cm^{-1}$) in DMF. Such absorption bands arise from the d_π(Ru) → π^*(NO) transition.[33,40,46] It has already been shown that photoexcitation of this band leads to photorelease of NO from these ruthenium nitrosyls. The location of this transition in the UV region however restricts the photosensitivity of typical {Ru−NO}^{6} nitrosyls to UV light only. We have previously reported that change of Me_2bpb^{2-} ligand

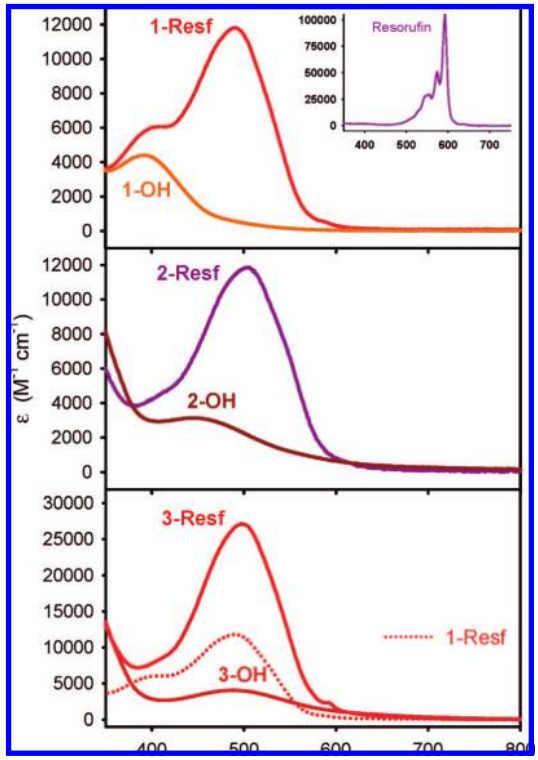

Figure 4. Electronic absorption spectra of **1-Resf** and **1-OH** (top), **2-Resf** and **2-OH** (middle) and **3-Resf** and **3-OH** (bottom panel) in DMF. Inset of top panel: electronic absorption spectrum of the unbound dye Resf (Na salt) in DMF. In the bottom panel, the spectrum of **1-Resf** is included again to show the merging of the photoband with the dye band in **3-Resf**.

to Me_2bQb^{2-} red shifts the photoband of the resulting nitrosyl to 450 nm (in DMF).[31] In the present work, we have synthesized a new ligand $H_2(OMe)_2bQb$ which affords the nitrosyl [((OMe)$_2$bQb)Ru(NO)(OH)] (**3-OH**). The red solution of this nitrosyl in DMF displays its photoband at 490 nm, although the extinction coefficient decreases to some extent ($\epsilon \approx 4\ 000$ $M^{-1}\ cm^{-1}$). Collectively, these results strongly suggest that the d_π(Ru) $\rightarrow$ π^*(NO) transition (photoband) of a {Ru−NO}^{6} nitrosyl can be modulated via alterations in the ligand frame.

Effective photoexcitation of a ruthenium nitrosyl by visible light requires (a) a photoband in the visible region and (b) significant absorption of visible light (high extinction coefficient). In order to impart significant absorption in the visible region, we now show that direct coordination of a dye molecule to the ruthenium center does increase the extinction coefficient of nitrosyls of the type [(R$_2$byb)Ru(NO)(L)]. As shown in the top panel of Figure 4, the bright red solution of [(Me$_2$bpb)Ru(NO)(Resf)] (**1-Resf**) in DMF exhibits a very strong absorption at 500 nm ($\epsilon = 12\ 000\ M^{-1}\ cm^{-1}$) arising from the directly coordinated dye molecule. **1-Resf** also displays its intrinsic d_π(Ru) $\rightarrow$ π^*(NO) transition as a shoulder at 395 nm ($\epsilon = 6\ 000\ M^{-1}\ cm^{-1}$), which closely corresponds to an analogous transition in **1-OH** ($\lambda_{max} = 390$ nm; $\epsilon = 5\ 100\ M^{-1}\ cm^{-1}$). Together, the nitrosyl-dye conjugate **1-Resf** exhibits much enhanced absorption in the visible range compared to nitrosyls like **1-OH** and as discussed below, such sensitization greatly improves the photosensitivity of **1-Resf** to visible light.

It is interesting to note that the bound dye moiety in **1-Resf** exhibits markedly different absorption features than that of unbound Resf.[44,45] The electronic absorption spectrum of unbound Resf (sodium salt) in DMF (dark violet solution) is dominated by a sharp, intense band at 590 nm ($\epsilon = 105\ 000$ $M^{-1}\ cm^{-1}$).[45] This absorption band has been shown to arise from the $\pi \rightarrow \pi^*$(Resf) transition. Its location in the low energy region (~600 nm) region has its origin in the low-lying, delocalized π^*-system of the heterocyclic ring system of Resf anion. The $\pi \rightarrow \pi^*$(ring) transition is strongly favored both by the selection rules and the high symmetry of the deprotonated Resf moiety.[44] The absorption spectrum of **1-Resf** clearly indicates that the electronic structure of Resf is greatly perturbed upon coordination to the ruthenium center. First, the observed transition of the dye is significantly blue-shifted (from 600 to 500 nm). Second, the intensity of the transition is greatly reduced (from 105 000 $M^{-1}\ cm^{-1}$ to 12 000 $M^{-1}\ cm^{-1}$). Direct coordination of the phenolato oxygen of Resf anion to the ruthenium center shifts the dye band to higher energy. Loss of symmetry upon coordination of Resf to ruthenium is most possibly responsible for the reduction of the extinction coefficient of the dye band in **1-Resf**. A similar blue shift of the absorption maximum and loss of intensity are observed when the phenolato oxygen of Resf is methylated (λ_{max} of Me-Resf = 460 nm in DMF, $\epsilon = 16\ 200\ M^{-1}\ cm^{-1}$).

Close examination of the absorption spectrum of **1-Resf**, however, reveals that the photoband of the {Ru−NO}^{6} core is still somewhat distinct from the dye band of Resf. In order to bring the λ_{max} of the photoband further into the dye absorption, we have attached Resf to {(Me$_2$bQb)Ru(NO)} and {((OMe)$_2$bQb)Ru(NO)}moieties to isolate [(Me$_2$bQb)Ru(NO)(Resf)] (**2-Resf**) and [((OMe)$_2$bQb)Ru(NO)(Resf)] (**3-Resf**) respectively. As shown in Figure 4, the photoband of the {Ru−NO}^{6} core does merge with the dye band systematically as one moves from **1-Resf** to **2-Resf** to **3-Resf**. The absorption spectra of [(Me$_2$bQb)Ru(NO)(OH)] (**2-OH**) and [((OMe)$_2$bQb)Ru(NO)(OH)] (**3-OH**) (also shown in Figure 4) clearly indicate the location of the intrinsic photoband of the {Ru−NO}^{6} core in the latter cases. Complete merging of the photoband of the {Ru−NO}^{6} core into the absorption band of Resf in **3-Resf** generates *one* intense and symmetric band at 505 nm. Interestingly, the extinction coefficient of this nitrosyl-dye conjugate is much higher (28 000 $M^{-1}\ cm^{-1}$) than that noted for either **1-Resf** or **2-Resf** (~12 000 cm^{-1}). Taken together, the optical parameters of **3-Resf** clearly satisfy the requirements of a ruthenium nitrosyl that could be highly sensitive to visible light.

NO Photorelease with Visible Light. Unlike their parent {Ru−NO}^{6} [(R$_2$byb)Ru(NO)(L)] nitrosyls, the nitrosyl-dye conjugates are sensitive to *visible light*.[31] Rapid changes in the electronic absorption spectrum are noted when solutions of these nitrosyls are exposed to visible light ($\lambda_{irr} \geq 465$ nm) due photorelease of NO (vide infra). For example, when an aqueous solution of **1-Resf** is illuminated with visible light (≥465 nm), the dye absorption band at 500 nm red shifts incrementally to 520 nm and new absorption features at 750 and 360 nm are observed (Figure 5). Clean isosbestic points at 320, 420, and 530 nm are also noted. Both the 750 and 360 nm band arise from the Ru(III) photoproduct (eq 1). This assignment is confirmed by the fact that both bands (760 and 365 nm) are observed upon photolysis of [(Me$_2$bpb)Ru(NO)(OH)] (**1-OH**)

(46) (a) Sizova, O. V.; Ivanova, N. V.; Sizov, W.; Nikol'skii, A. B. *Russ. J. Gen. Chem.* **2004**, *74*, 481–485. (b) Sizova, O. V.; Lyubimova, O. O.; Sizov, W. *Russ. J. Gen. Chem.* **2004**, *74*, 317–322. (c) Sizova, O. V.; Ivanova, N. V.; Lyubimova, O. O.; Nikol'skii, A. B. *Russ. J. Gen. Chem.* **2004**, *74*, 155–163. (d) Gorelsky, S. I.; da Silva, S. C.; Lever, A. B. P.; Franco, D. W. *Inorg. Chim. Acta* **2000**, *300*−*302*, 698–708. (e) Schreiner, A. F.; Lin, S. W.; Hauser, P. J.; Hopcus, E. A.; Hamm, D. J.; Gunter, J. D. *Inorg. Chem.* **1972**, *11*, 880–888.

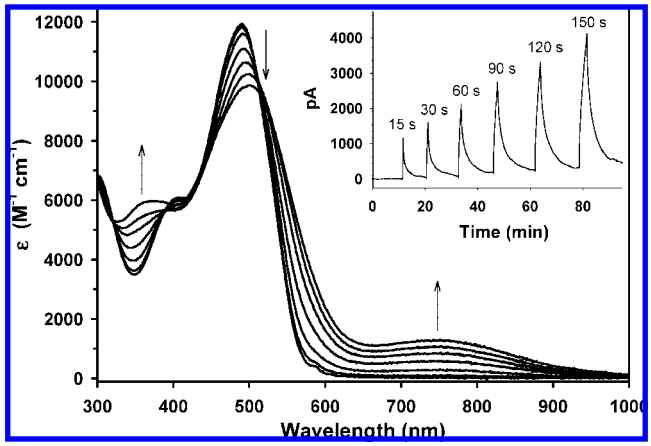

Figure 5. Changes in the electronic absorption spectra of **1-Resf** in water upon exposure to visible light ($\lambda_{irr} \geq 465$ nm; measured intensity: 300 mW). Note the clean isosbestic points at 320, 420, and 530 nm, as well as new peaks generated at 520 and 750 nm. Inset: NO amperogram trace of **1-Resf** in aqueous solution upon exposure to short pulses (as indicated) of visible light.

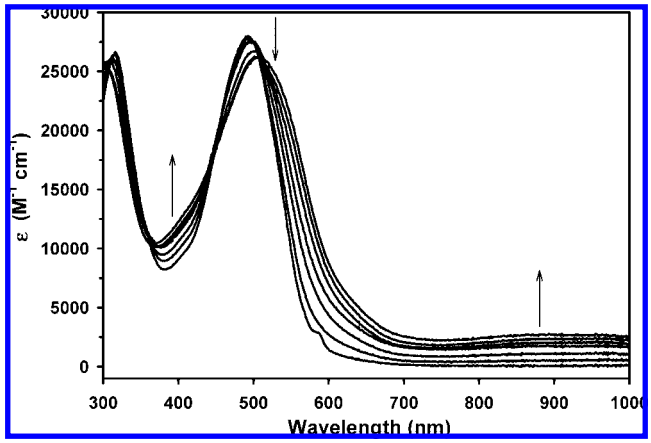

Figure 6. Changes in the electronic absorption spectra of **3-Resf** in MeCN upon exposure to visible light ($\lambda_{irr} \geq 465$ nm; measured intensity: 300 mW). Note the clean isosbestic points at 310, 360, 450, and 520 nm, as well as new peaks generated at 510 and 870 nm.

with UV light in DMF (Figure S2, Supporting Information). The low energy band near 700 nm, also noted in case of photolysis of [(salen)Ru(NO)(Cl)] with UV light, has been assigned to a ligand-to-metal charge-transfer (LMCT) band of the Ru(III) photoproduct (eq 1) by us and others.[31,40]

As mentioned above, merging of the photoband of the parent nitrosyl [((OMe)$_2$bQb)Ru(NO)(OH)] (**3-OH**) with the dye absorption band in **3-Resf** (Figure 4) results in an enhanced 500 nm absorption. When a solution of **3-Resf** in MeCN is exposed to visible light, this band red shifts to 510 nm, and a broad absorption feature at 870 nm is observed (Figure 6). Isosbestic points are noted at 310, 360, 450, and 520 nm. It is interesting to note that the LMCT band of the Ru(III) photoproduct namely, [((OMe)$_2$bQb)Ru(MeCN)(Resf)], shifts to 870 nm (Figure 6) as expected on the basis of the increased electron density in the equatorial ligand plane due to the −OMe groups compared to the −Me groups in [(Me$_2$bpb)Ru(MeCN)(Resf)] (exhibiting band at 750 nm in Figure 5). In addition, the ∼360 nm band of the Ru(III) photoproduct from **3-Resf** is also red-shifted and thus obscured by the intense dye absorption around 500 nm.

Formation of Ru(III) photoproducts upon NO photorelease ($\lambda_{irr} \geq 465$ nm) from the nitrosyl-dye conjugates **1-Resf**−**3-Resf** has been confirmed by EPR spectroscopy. The photoproduct of **1-Resf** in frozen DMF/toluene glass at 125 K exhibits a rhombic, low-spin signal ($g = 2.35$, 2.18, and 1.87), characteristic of a paramagnetic d^5 Ru(III) system (Figure S3, Supporting Information). The rhombic EPR signal arises from the solvated (DMF-bound) photoproduct [(Me$_2$bpb)Ru^{III}-(DMF)(Resf)]. The other two nitrosyl-dye conjugates (**2-Resf** and **3-Resf**) also exhibit nearly identical EPR spectra (Figure S3) after photolysis with visible light ($\lambda_{irr} \geq 465$ nm). In addition, UV photolysis of the hydroxide-bound species **1-OH**, **2-OH** and **3-OH** affords similar rhombic, low-spin Ru(III) signal. These results strongly suggest that our dicarboxamide ligands facilitate clean conversion of all of these {Ru−NO}^{6} nitrosyls to NO• and Ru(III) photoproducts (eq 1). To confirm the homolytic cleavage of the Ru−NO bond to form Ru(III) and NO• radical, we have also measured the amounts of liberated NO from the nitrosyl-dye conjugates with the aid of an NO-sensitive electrode (*ami*-NO 2000). As shown in the inset of Figure 5, illumination of **1-Resf** (∼0.1 mM) in aqueous solution with incremental pulses of visible light generates increasing amounts of photoreleased NO in solution. Such measurements with all three nitrosyl-dye conjugates confirm that *visible light photolysis* results in rapid release of NO in all cases. When compared with **1-OH**−**3-OH** (Table 3), it becomes evident that the coordinated dye ligand (Resf) imparts photosensitivity to visible light in these nitrosyl-dye conjugates. Collectively, the present results unequivocally demonstrate that the {Ru−NO}^{6} nitrosyls of the type [(X$_2$byb)Ru(NO)(L)] (X = H, Me, OMe; y = p (pyridine), Q (quinoline); L = Cl$^-$, py, OH$^-$) can be sensitized via substitution of L with Resf as the light-harvesting chromophore. In order to quantitatively assess the efficiency of NO release from this set of nitrosyl-dye conjugates, we have determined the quantum yields (ϕ) of NO release upon exposure to 500 nm light. The ϕ_{500} values obtained in such photolysis experiments with monochromatic *visible* light are listed in Table 3. The present sets of dye- and hydroxide-bound nitrosyls present a unique opportunity to unambiguously assess the effect of dye coordination upon visible-light driven NO release. Under 500 nm illumination, **1-Resf** exhibits a moderate quantum yield of $\phi_{500} = 0.052 \pm 0.008$. This value compares quite well to other ruthenium nitrosyls studied in the visible region so far. For example, a ϕ_{532} value of 0.025 ± 0.002 has been reported for the dinuclear {Ru−NO}^{6} nitrosyl [Ru(NH$_3$)$_5$(pz)Ru(bpy)$_2$(NO)](PF$_6$)$_5$ by Da Silva and co-workers.[47] An increasing degree of overlap between the absorption band of Resf and the photoband of the nitrosyl moiety in the case of **2-Resf** and **3-Resf** (Figure 4) further enhances their quantum yield values at 500 nm. For example, the ϕ_{500} values of **2-Resf** and **3-Resf** are nearly 2× (0.102 ± 0.009) and 4× (0.206 ± 0.008) that of **1-Resf** (Table 3).

Our strategy of *direct coordination* of the light-harvesting chromophore Resf to the metal centers affords a higher degree of enhancement in NO photolability compared to the *pendant chromophore* approach reported by Ford and co-workers. This group has derivatized Roussin's salts with fluorescein (Fluor-

(47) (a) Sauaia, M. G.; de Lima, R. G.; Tedesco, A. C.; da Silva, R. S. *Inorg. Chem.* **2005**, *44*, 9946–9951. (b) Sauaia, M. G.; de Lima, R. G.; Tedesco, A. C.; da Silva, R. S. *J. Am. Chem. Soc.* **2003**, *125*, 14718–14719.

Table 3. Summary of Visible Absorption Spectra (λ_{max}) and Quantum Yield (ϕ) Values (in visible range) of Selected Nitrosyls Discussed in This Work

complex	quantum yield ϕ (λ_{irr}, nm)	solvent	λ_{max}, nm ϵ, M^{-1} cm^{-1})
[(Me_2bpb)Ru(NO)(Resf)] (**1-Resf**)	0.052 ± 0.008 (500)	DMF	500 (11 920)
[(Me_2bQb)Ru(NO)(Resf)] (**2-Resf**)	0.102 ± 0.009 (500)	DMF	510 (12 300)
[((OMe)$_2$bQb)Ru(NO)(Resf)] (**3-Resf**)	0.206 ± 0.008 (500)	DMF	500 (27 100)
[(Me_2bpb)Ru(NO)(OH)](**1-OH**)	0.0008 ± 0.0002 (500)	DMF	390 (5 100)
[(Me_2bQb)Ru(NO)(OH)] (**2-OH**)	0.010 ± 0.003 (500)	DMF	445 (3 130)
[((OMe)$_2$bQb)Ru(NO)(OH)] (**3-OH**)	0.025 ± 0.003 (500)	DMF	490 (4 060)
[(Py_3P)Ru(NO)]BF_4[a]	0.050 ± 0.004 (532)	MeCN	530 sh (400)
[$Ru(NH_3)_5$(pz)Ru(bpy)$_2$(NO)]$(PF_6)_5$[b]	0.025 ± 0.002 (532)	H_2O (4.5)	530 (9 550)
[($PaPy_3$)Mn(NO)]ClO_4[c]	0.385 ± 0.010 (550)	H_2O (7.4)	635 (220)
[($PaPy_3$)Fe(NO)]$(ClO_4)_2$[d]	0.185 ± 0.003 (500)	MeCN	500 (1 050)
Roussin's Red Salt (RRS)[e]	~0.13 (546)	H_2O (7)	374 (10 400)
Roussin's Salt Ester (RSE)[f]	0.00019 ± 0.00005(546)	$CHCl_3$	364 (8 500)
PPIX-RSE[g]	0.00025 ± 0.00005(546)	$CHCl_3$	538 (10 200)
Fluor-RSE[h]	0.0036 ± 0.0005(436)	MeCN/H_2O (7.4)	506 (72 200)

[a] ref 39a. [b] ref 48. [c] ref 51a. [d] ref 51b. [e] ref 23b. [f] ref 21a. [g] ref 49b. [h] ref 48b.

RSE)[48] or protoporphyrin IX (PPIX-RSE).[49] The light-harvesting chromophores in these conjugates are, however, tethered to the metal centers (bearing NO ligands) via alkyl linkers. As a result, they release NO less efficiently when exposed to light (Table 3). When peripheral UV antennae are tethered to the ligand frame of NO-releasing complexes such as *trans*-[(cyclam-L)Cr(ONO)$_2$]BF_4 (antennae L = pyrene, anthracene), the intrinsic quantum yield of NO production remains unchanged.[50] The quantum yield values of Table 3 clearly attest that our strategy of direct coordination of chromophore is superior in enhancing the NO photolability of metal nitrosyls.

Although solutions of free Resf in DMF and water are highly fluorescent (λ_{ex} = 590 nm, λ_{em} ≈ 610 nm) at room temperature, **1-Resf**- **3-Resf** exhibit strongly quenched (~90% quenched) fluorescence emission due to energy transfer between the coordinated dye and the Ru−NO moiety.[52,53] For example, a solution of **1-Resf** in aqueous phosphate buffer (pH 7.4) at room temperature exhibits a broad red fluorescence emission band of low intensity at 580 nm (Figure S4, Supporting Information). The residual fluorescence of the nitrosyl-dye conjugates is however sufficient for their successful use as "trackable NO donors". As discussed in the following section, these photoactive NO donors allow one to follow them during targeted NO delivery in a cellular environment.

Another desirable property of these nitrosyl-dye conjugates arises from the fact that their fluorescence is quenched upon photorelease of NO due to the presence of paramagnetic Ru(III) center in the photoproducts. In other words, these trackable NO donors possess an On/Off switch. As shown in Figure 7, progressive loss of NO from **1-Resf** upon exposure to light causes systematic quenching of the fluorescence of the Resf moiety. The sample shown in Figure 7 lost all NO by the end of 3 min. This transformation can also be followed by systematic changes in its absorption spectrum (as shown in Figure 5). Since the two processes follow the same time course in either measurement, it is evident that the extent of fluorescence quenching is directly related to the degree of NO loss in this set of nitrosyl-dye conjugates.

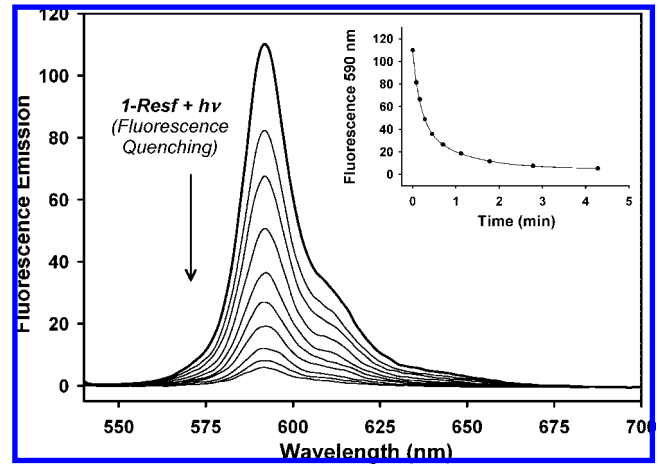

Figure 7. Changes in the fluorescence emission of **1-Resf** in MeCN (λ_{ex} = 530 nm) following exposure to visible light (λ_{irr} ≥ 465 nm; measured intensity: 300 mW). Inset: time course of loss of fluorescence following NO photorelease.

NO delivery to Cellular Targets using Visible Light. The unusual capacity of rapid NO release under visible light combined with appreciable fluorescence makes the present nitrosyl-dye conjugates (**1-Res–3-Resf**) ideal candidates for use in studying NO-induced apoptosis in tumor cells. One can not only "track" these NO donors in the intracellular environment of malignant cells via fluorescence microscopy, but selectively "trigger" them by an external stimulus (visible light) and monitor the apoptotic effect(s) of high doses of NO inside the target cells. In the present work, we have tested this hypothesis by using **1-Resf** as the NO donor and human mammary cancer MDA-MB-231 cells. Other groups have already demonstrated that MDA-MB-231 cells undergo apoptosis in the presence of

(48) (a) Wecksler, S. R.; Mikhailovsky, A.; Korystov, D.; Ford, P. C. *J. Am. Chem. Soc.* **2006**, *128*, 3831–3837. (b) Wecksler, S. R.; Hutchinson, J.; Ford, P. C. *Inorg. Chem.* **2006**, *45*, 1192–1200.
(49) (a) Baker, E. S.; Bushnell, J. E.; Wecksler, S. R.; Lim, M. D.; Manard, M. J.; Dupuis, N. F.; Ford, P. C.; Bowers, M. T. *J. Am. Chem. Soc.* **2005**, *127*, 18222–18228. (b) Conrado, C. L.; Wecksler, S.; Egler, C.; Magde, D.; Ford, P. C. *Inorg. Chem.* **2004**, *43*, 5543–5549.
(50) (a) DeRosa, F.; Bu, X.; Ford, P. C. *Inorg. Chem.* **2005**, *44*, 4157–4165. (b) DeRosa, F.; Bu, X.; Pohaku, K.; Ford, P. C. *Inorg. Chem.* **2005**, *44*, 4166–4174. (c) DeRosa, F.; Bu, X.; Ford, P. C. *Inorg. Chem.* **2003**, *42*, 4171–4178.
(51) (a) Eroy-Reveles, A. A.; Leung, Y.; Beavers, C.; Olmstead, M. M.; Mascharak, P. K. *J. Am. Chem. Soc.* **2008**, (b) Eroy-Reveles, A. A.; Hoffman-Luca, C. G.; Mascharak, P. K. *Dalton Trans.* **2007**, 5268–5274.
(52) Turro, N. J. *Modern Molecular Photochemistry*; University Science: Mill Valley, USA, 1991.
(53) (a) Sapsford, K. E.; Berti, L.; Medintz, I. L. *Angew. Chem., Int. Ed.* **2006**, *45*, 4562–4588. (b) Raymo, F. M.; Tomasulo, M. *Chem. Soc. Rev.* **2005**, *34*, 327–336. (c) Huynh, M. H. V.; Dattelbaum, D. M.; Meyer, T. J. *Coord. Chem. Rev.* **2005**, *249*, 457–483. (d) Faure, S.; Stern, C.; Guillard, R.; Harvey, P. D. *J. Am. Chem. Soc.* **2004**, *126*, 1253–1261.

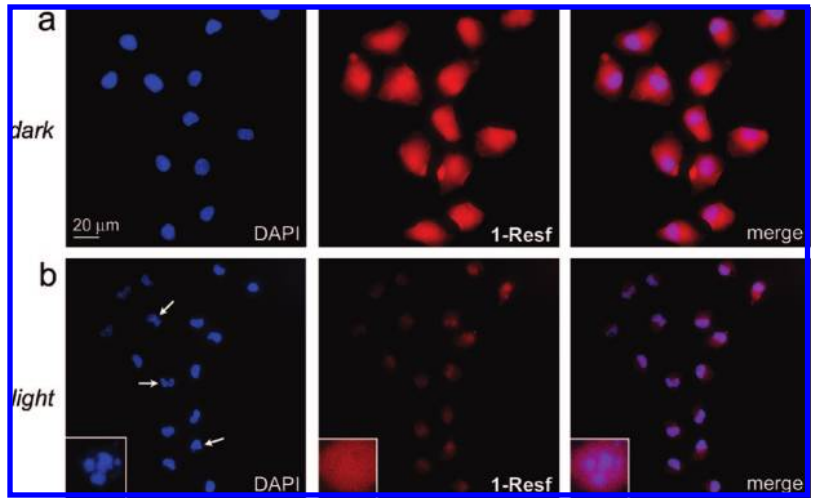

Figure 8. MDA-MB-231 cells were loaded with 200 μM solution of **1-Resf** in PBS-Ca/Mg for 1 h and either (a) kept in the dark or (b) exposed to 1 min visible light ($\lambda \geq 465$ nm, 0.3 W measured intensity); note the nuclear degradation (arrows). Bottom insets: magnified views of a cell undergoing apoptosis.

NO[54] or other stimuli like TNF-α and IFN-β.[55] The pyknotic nuclei of apoptotic cells are easily recognized by features such as chromatin condensation, nuclear budding, and loss of cytoplasm.

As shown in the panel a of Figure 8, **1-Resf** is readily taken up by live cells (1 h incubation at 37 °C) and its presence inside the cells is easily noted by the bright red fluorescence. This NO donor exhibits both cytosolic and nuclear staining patterns, which indicate a significant concentration of **1-Resf** within the cell. In contrast, control experiments with free Resf under identical conditions led only to nonspecific extracellular staining. These results confirm that the intact **1-Resf** is responsible for the observed red fluorescence. In order to check whether **1-Resf** loses Resf inside (or outside) the cell, we have studied the integrity of the nitrosyl-dye conjugate **1-Resf** in phosphate buffers of pH 5−8. In phosphate buffers of pH 6−8, **1-Resf** loses less than 5% of the bound dye in 1 h. Since the cells were incubated with **1-Resf** in phosphate buffer of pH 7.4, we believe that only minimal loss of Resf occured during the 1 h incubation. When the pH is lowered to 5, ∼10% of Resf is lost from **1-Resf** within 1 h. Clearly, the red fluorescence observed in the middle frame of panel **a** of Figure 8 arises mostly from intact **1-Resf**. Even after 4 h, only 15% loss of Resf from **1-Resf** is noted in phosphate buffer of pH 5. It is therefore evident that the major portion of **1-Resf** uptaken by the cells remains intact and ready to donate NO upon exposure to light.

Panel a of Figure 8 also show that cells loaded with **1-Resf** and incubated for up to 8 h *in the dark* exhibit no visible signs of apoptosis. However, brief exposure (1 min) of visible light ($\lambda \geq 465$ nm, 0.3 W) results in marked signs of apoptosis after 4−8 h. As shown in panel b of Figure 8 (arrows), light-exposed cells exhibit a significant extent of chromatin condensation (and fragmentation) and loss of cytoplasm. The red fluorescence is somewhat diminished in light-exposed cells due to partial loss of fluorescence via quenching by the paramagnetic ($S = 1/2$, d^5) Ru^{III} photoproduct generated upon NO release. No apoptotic morphologies are observed at earlier time points (1−2 h), consistent with other published timelines of NO-induced apoptosis. Additionally, in control experiments untreated cells exposed to visible light showed no irregular (apoptotic) morphologies, and remained healthy over the same time period.

Finally, we have employed the TUNEL (terminal dUTP nick end labeling) assay to demonstrate the apoptotic signaling cascade induced by **1-Resf** in light-exposed MDA-MB-231 cells.[56] This method labels cleaved DNA in apoptotic cells with a green fluorescein-based nucleotide, whereas nonapoptotic cells (with intact DNA) remain unstained. As shown in panel **a** of Figure 9, cells treated with **1-Resf**, but kept in the dark do not exhibit TUNEL staining. However, light-exposed cells exhibit positive TUNEL staining (panel **b**, Figure 9). In the merged image (far right), the red fluorescence in conjunction with the green TUNEL labeling clearly distinguishes apoptotic from adjacent nonapoptotic cells on an individual cell basis (see arrows). Additionally, the observed timeline of apoptosis (as shown in Figure 10) shows significant cellular degradation ($p < 0.05$; *t*-test) at 4 to 8 h, consistent with the reported timelines of apoptosis observed with this cell line[57a] as well as others.[57b] At 8 h, apoptotic cells display loss of adherence, which may account for the slight decrease between 4 and 8 h (Figure 10).

Taken together, the data presented here demonstrate that **1-Resf** initiates apoptosis in MDA-MB-231 cells when triggered by visible light. It is evident that **1-Resf** can be "tracked" in a targeted area before it begins NO photorelease. In contrast, conventional NO donors with a tag of this kind[58] would release NO spontaneously in the extracellular matrix (not trackable), and the resulting diffusion of NO would limit the specificity of the action of the drug (NO donor). At this time, we are pursuing more experiments to compare the efficacies of all three nitrosyl-dye conjugates in MDA-MB-231 and other cancer cell lines.

(54) Simeone, A.-M.; Colella, S.; Krahe, R.; Johnson, M. M.; Mora, E.; Tari, A. M. *Carcinogenesis.* **2006**, *27*, 568–577.
(55) Kang, J. X.; Liu, J.; Wang, J. D.; He, C. W.; Li, F. P. *Carcinogenesis.* **2005**, *26*, 1934–1939.
(56) (a) Thangapazham, R. L.; Singh, A. K.; Sharma, A.; Warren, J.; Gaddpati, J. P.; Maheshwari, R. K. *Cancer Letts.* **2007**, *245*, 232–241. (b) Kim, M.; Katayose, Y.; Rojanala, L.; Shah, S.; Sgagias, M.; Jang, L.; Jung, Y.-L.; Lee, S.-H.; Hwang, S.-G.; Cowan, K. H. *Cell Death Differ.* **2000**, *7*, 706–711.
(57) (a) Viale, M.; Mariggio, M. A.; Ottone, M.; Chiavarina, B.; Vinella, A.; Prevesto, C.; Dell'Arba, C.; Petrillo, G.; Novi, M. *Invest. New Drugs.* **2004**, *22*, 359–267. (b) Meβner, U. K.; Brüne, B. *Arch. Biochem. Biophys.* **1996**, *327*, 1–10.
(58) (a) Tannous, M.; Hutnik, C. M. L.; Tingey, D. P.; Mutus, B. *Invest. Opthamol. Vis. Sci.* **2000**, *41*, 749–755. (b) Saavedra, J. E.; Booth, M. N.; Hrabie, J. A.; Davies, K. M.; Keefer, L. K. *J. Org. Chem.* **1999**, *64*, 5124.

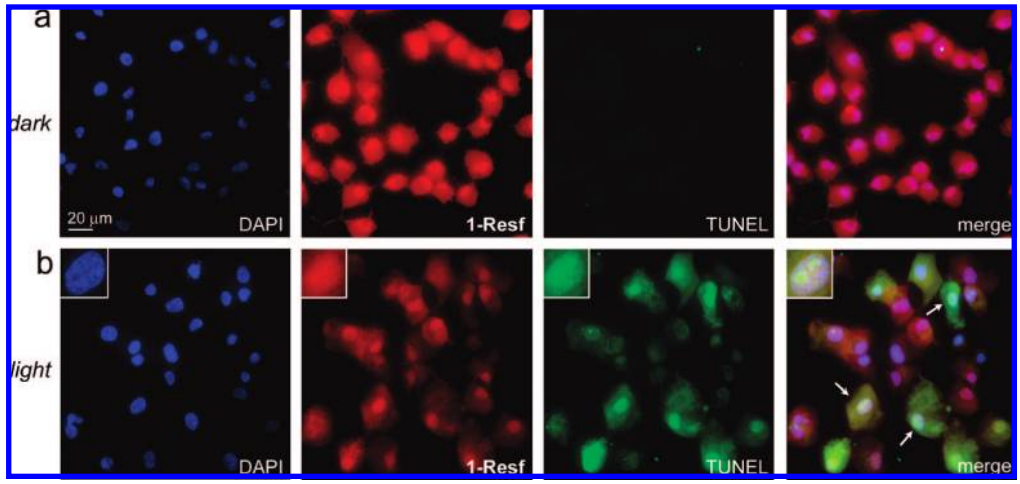

Figure 9. Fluorescence microscopy of apoptotic MDA-MB-231 cells treated with 200 μM **1-Resf** and either (a) kept in the dark or (b) exposed to 1 min visible light ($\lambda \geq 465$ nm, 0.3 W). Insets: magnified views of an apoptotic cell showing TUNEL-detected DNA fragmentation.

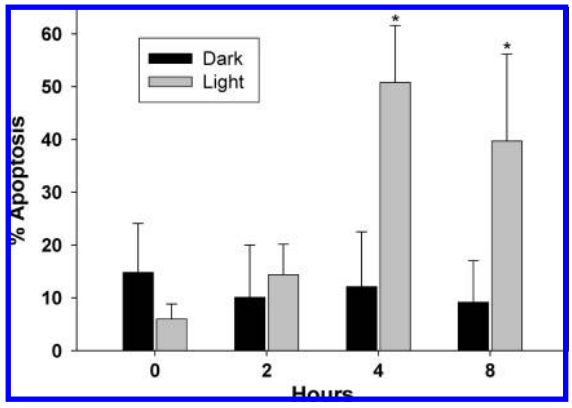

Figure 10. Timeline of apoptosis observed in MDA-MB-231 cells treated with 200 μM **1-Resf** and kept in the dark, or exposed to 1 min visible light ($\lambda \geq 465$ nm, 0.3 W). Apoptotic cells displaying blebbing, pyknotic nuclei, or nuclear decomposition were counted versus healthy cells (mean $\pm$ s.d. is shown). Asterisks (*) indicate significant difference ($p < 0.05$; *t*-test) between light-exposed and dark samples, and at least ten fields of view were counted in each case.

Overall, we show that **1-Resf** and its congeners exhibit a remarkable convergence of useful properties—aqueous solubility and stability, photoactivation with visible light, trackable fluorescence, and membrane permeability, all of which are crucial for using these NO donors as tools in biological research. For example, fluorescent NO donors such as **1-Resf** could aid in the cellular imaging of NO-dependent pathways via fluorescence microscopy.

Recent advances in photodynamic therapy (PDT) have allowed a higher degree of tissue selectivity in cancer therapy.[15] In addition, some newer PDT agents have been designed with trackable fluorophores, enabling tumor identification and fluorescence-guided resection (FGR).[59] Unfortunately, many current PDT agents like porphyrins and phthalocyanins induce oxidative cell death through generation of singlet oxygen ($^1O_2$) and other reactive oxygen species (ROS).[15] In such cases, cell death occurs via necrosis, a process that generates a host immune response and undesirable inflammatory side effects.[60] Apoptosis, on the other hand, does not elicit such a response, and is thus more tolerable to the patient. A "trackable" NO donor that could be triggered by selective stimulus like light to induce apoptotic cell death will therefore be a very desirable tumor-specific PDT drug.

Conclusions

The following are the summary and conclusions of the present work:

(1) A set of nitrosyl-dye conjugates **1-Resf**−**3-Resf** in which the dye resorufin (Resf) is directly coordinated to the ruthenium centers of the $\{Ru-NO\}^6$ nitrosyls [(R_2byb)Ru(NO)(Cl)] has been synthesized via replacement of the chloride ligand with the anionic resorufin dye. The structures of these nitrosyl-dye conjugates have been determined by X-ray crystallography. In all three species, the dye is bonded to the ruthenium center via the phenolato-O atom, trans to NO. These nitrosyl-dye conjugates are thermally stable solids and dissolve in solvents like MeCN and DMF. They are also moderately soluble in water.

(2) Careful selection of R and y group in the parent tetradentate equatorial ligand R_2byb^{2-} allows red shift of the $d_\pi(Ru) \rightarrow \pi^*(NO)$ transition (photoband) of the parent nitrosyls from 380 to 500 nm. Such red shift results in an eventual coalescing of the photoband with the intense dye absorption in the visible range (~500 nm) as one moves from **1-Resf** to **2-Resf** to **3-Resf**. **3-Resf** exhibits one strong absorption band ($\epsilon = 28\ 000\ M^{-1}\ cm^{-1}$) at 500 nm.

(3) The light-harvesting dye chromophore sensitizes the otherwise UV-sensitive nitrosyls toward visible light. As a consequence, the nitrosyl-dye conjugates rapidly release NO when exposed to visible light ($\lambda \geq 465$ nm) of moderate intensity (0.3 W). Photochemical parameters of these photosensitive NO donors clearly indicate that direct coordination of the dye chromophore to the ruthenium center affords a much higher degree of sensitization compared to nitrosyls with appended chromophores (linked via alkyl chains).

(59) (a) Kamiya, M.; Kobayashi, H.; Hama, Y.; Koyama, Y.; Bernardo, M.; Nagano, T.; Choyke, P. L.; Urano, Y. *J. Am. Chem. Soc.* **2007**, *129*, 3918–3929. (b) Leevy, W. M.; Gammon, S. T.; Jiang, H.; Johnson, J. R.; Maxwell, D. J.; Jackson, E. N.; Marquez, M.; Piwnica-Worms, D.; Smith, B. D. *J. Am. Chem. Soc.* **2006**, *128*, 16476–16477. (c) Bogaards, A.; Zhang, K.; Zach, D.; Bisland, S. K.; Moriyama, E. H.; Lilge, L.; Muller, P. J.; Wilson, B. C. *Photochem. Photobiol. Sci.* **2005**, *4*, 438–442.

(60) (a) Korbelik, M. *Lasers Surg. Med.* **2006**, *38*, 500–508. (b) Castano, A. P.; Mroz, P.; Hamblin, M. R. *Nat. Rev. Cancer.* **2006**, *6*, 535–545. (c) Lilge, L.; Portnoy, M.; Wilson, B. C. *Br. J. Cancer* **2000**, *83*, 1110–1117.

(4) Since all nitrosyl-dye conjugates exhibit significant fluorescence, it is possible to "track" these photosensitive NO donors in the cellular environment with the aid of fluorescence microscopy. As a proof-of-concept experiment, **1-Resf** has been employed to promote NO-induced apoptosis in MDA-MB-231 human breast cancer cells and the NO donor has been tracked during the process of programmed cell death. Collectively, the results indicate that ruthenium nitrosyls could be sensitized to visible light via direct coordination of dye chromophores to the metal center and such nitrosyl-dye conjugates could be used as "trackable" NO donors in the PDT of malignancies (such as skin cancer).

Acknowledgment. This work was supported by a grant from the National Science Foundation (CHE-0553405). The X-ray diffraction facility at UCSC is supported by the NSF instrumentation grant CHE-0521569. M.J.R. gratefully acknowledges the UCSC Graduate Division for a Dissertation Year Fellowship. Experimental assistance in structure determination from Dr. Marilyn Olmstead and Dr. Allen Oliver is gratefully acknowledged. We also thank Prof. Theodore Holman for allowing us the generous use of fluorescence instrumentation.

Supporting Information Available: Thermal ellipsoid plot of **1-OH** (Figure S1), changes in electronic absorption spectrum upon UV photolysis of **1-OH** and **3-OH** in DMF (Figure S2), X-band EPR spectra of photoproducts of **1-Resf** and **3-Resf** (frozen DMF/toluene glass, Figure S3), fluorescence emission spectrum of **1-Resf** in aqueous phosphate (pH 7.4) buffer (Figure S4), X-ray crystallographic data (in CIF format) for the structure determination of **1-OH**·DMSO, **1-Resf**·H_2O, **2-Resf**·$CHCl_3$, and **3-Resf**. This material is available free of charge via the Internet at http://pubs.acs.org.

JA801823F